Leukemia-associated activating mutation of Flt3 expands dendritic cells and alters T cell responses

Colleen M. Lau,[1,2,3] Simone A. Nish,[3] Nir Yogev,[4] Ari Waisman,[4] Steven L. Reiner,[3] and Boris Reizis[1,2,3]

[1]Department of Pathology and [2]Department of Medicine, New York University Langone Medical Center, New York, NY 10016
[3]Department of Microbiology and Immunology, Columbia University Medical Center, New York, NY 10032
[4]Institute for Molecular Medicine, University Medical Center of the Johannes Gutenberg-University of Mainz, Mainz 55131, Germany

A common genetic alteration in acute myeloid leukemia is the internal tandem duplication (ITD) in FLT3, the receptor for cytokine FLT3 ligand (FLT3L). Constitutively active FLT3-ITD promotes the expansion of transformed progenitors, but also has pleiotropic effects on hematopoiesis. We analyzed the effect of FLT3-ITD on dendritic cells (DCs), which express FLT3 and can be expanded by FLT3L administration. Pre-leukemic mice with the *Flt3*^{ITD} knock-in allele manifested an expansion of classical DCs (cDCs) and plasmacytoid DCs. The expansion originated in DC progenitors, was cell intrinsic, and was further enhanced in *Flt3*$^{ITD/ITD}$ mice. The mutation caused the down-regulation of Flt3 on the surface of DCs and reduced their responsiveness to Flt3L. Both canonical Batf3-dependent CD8$^+$ cDCs and noncanonical CD8$^+$ cDCs were expanded and showed specific alterations in their expression profiles. *Flt3*^{ITD} mice showed enhanced capacity to support T cell proliferation, including a cell-extrinsic expansion of regulatory T (T reg) cells. Accordingly, these mice restricted alloreactive T cell responses during graft-versus-host reaction, but failed to control autoimmunity without T reg cells. Thus, the FLT3-ITD mutation directly affects DC development, indirectly modulating T cell homeostasis and supporting T reg cell expansion. We hypothesize that this effect of FLT3-ITD might subvert immunosurveillance and promote leukemogenesis in a cell-extrinsic manner.

Activating mutations of Fms-like tyrosine kinase 3 (Flt3) comprise up to ∼30% of genetic lesions found in acute myeloid leukemia (AML), making it one of the most frequently mutated genes in AML. The most common of these activating mutations is the Flt3 internal tandem duplication (FLT3-ITD), which yields a constitutively active receptor. The acquisition of FLT3-ITD is strongly associated with increased risk of relapse and decreased overall survival (Kindler et al., 2010; Swords et al., 2012). Recent genome-wide sequencing studies confirmed the common occurrence of FLT3-ITD and revealed its appearance and persistence in the founding leukemic clone (Ding et al., 2012; Jan et al., 2012; Cancer Genome Atlas Research Network, 2013; Shlush et al., 2014). Genomic analysis of AML relapses revealed a selective pressure to maintain the kinase activity of FLT3-ITD, establishing it as a driver mutation (Smith et al., 2012).

The Flt3 receptor is expressed on early hematopoietic stem cells (HSCs) and progenitor cells during normal hematopoiesis (Adolfsson et al., 2001; Karsunky et al., 2003; Sitnicka et al., 2003). Flt3 binds a cytokine called Flt3 ligand (Flt3L) that is required for efficient lymphoid and myeloid development (McKenna et al., 2000), whereas long-term administration of exogenous Flt3L causes myeloproliferation (Brasel et al., 1996). The Flt3L–Flt3 signaling cascade activates multiple signal transduction pathways that ultimately promote survival and cell proliferation. Based on the expression pattern of Flt3 and functional consequences of its signaling, the Flt3-ITD mutation is thought to increase the survival and proliferation of transformed Flt3$^+$ progenitors (Parcells et al., 2006; Small, 2006). However, recent studies have uncovered additional effects of FLT3-ITD that may contribute to its leukemogenic effects. For instance, Flt3-ITD has been shown to abrogate the quiescence of HSCs, leading to their hyperproliferation and eventual exhaustion (Chu et al., 2012). In addition, Flt3-ITD promotes myelopoiesis at the expense of lymphopoiesis, in part by enforcing a myeloid-biased transcriptional program (Mead et al., 2013). To better understand and target the mechanism of FLT3-ITD–driven leukemogenesis, it is important to fully characterize the effects of FLT3-ITD on normal hematopoiesis.

In addition to early hematopoietic progenitors, Flt3 is expressed in a single mature hematopoietic lineage: DCs (Liu and Nussenzweig, 2010). DCs are mononuclear phagocytes that initiate adaptive immune responses, and are comprised of two major types: antigen-presenting classical DCs (cDCs) and type I IFN–producing plasmacytoid DCs (pDCs). All DCs develop in the BM from common DC progenitors (CDPs), which either generate mature pDCs in

Correspondence to Boris Reizis: Boris.Reizis@nyumc.org

Abbreviations used: AML, acute myeloid leukemia; cDC, classical DC; CDP, common DC progenitor; CTV, Cell Trace Violet; DT, diphtheria toxin; FLT3L, FLT3 ligand; GVHD, graft-versus-host disease; HSC, hematopoietic stem cell; ITD, internal tandem duplication; MLR, mixed leukocyte reaction; pDC, plasmacytoid DC.

The Rockefeller University Press $30.00
J. Exp. Med. 2016 Vol. 213 No. 3 415–431
www.jem.org/cgi/doi/10.1084/jem.20150642

situ or give rise to committed cDC progenitors (preDCs; Geissmann et al., 2010). The latter exit into the periphery and undergo differentiation into two main cDC subsets: the $CD8^+/CD103^+$ cDCs capable of antigen cross-presentation, and $CD11b^+$ (myeloid) DCs that efficiently present exogenous antigens. The phenotype, transcriptional control, and functionality of the main DC subsets are conserved between experimental animals and humans (Merad et al., 2013). DCs are highly efficient in priming antigen-specific T cell responses; conversely, in the steady-state they are thought to promote antigen-specific T cell tolerance. This tolerogenic function of DCs may include the induction of T cell unresponsiveness, as well as the maintenance of regulatory T cells (T reg cells; Steinman et al., 2003; Lewis and Reizis, 2012). These mechanisms are particularly important in the context of cancer, as DCs can be hijacked to establish immunosuppressive microenvironments to promote tumorigenesis (Maldonado and von Andrian, 2010).

Genetic ablation of Flt3L severely impairs DC development (McKenna et al., 2000), whereas the deletion of Flt3 causes specific defects in tissue DCs (Waskow et al., 2008; Ginhoux et al., 2009). Conversely, Flt3L administration dramatically increases the number of DCs in both mice and humans (Maraskovsky et al., 1996, 2000; Breton et al., 2015). Consistent with the tolerogenic role of DCs in the steady state, Flt3L-mediated DC expansion appears to dampen immune responses. In particular, in vivo Flt3L administration was shown to increase the T reg cell population, attenuate tissue inflammation and protect from T cell-mediated graft-versus-host disease (GVHD; Chilton et al., 2004; Darrasse-Jèze et al., 2009; Swee et al., 2009; Collins et al., 2012). Thus, Flt3 activation directly expands Flt3-expressing DCs and their progenitors, thereby indirectly modulating T cell homeostasis and creating a tolerogenic environment.

Given that the FLT3-ITD mutation activates Flt3 signaling, we hypothesized that it may directly affect the DC lineage in a manner similar to Flt3L administration. In this study, we analyzed DC development and immune homeostasis in the mouse strain with a germ-line ITD mutation in the endogenous *Flt3* locus. We report that heterozygous and homozygous Flt3-ITD mutations cause a progressive expansion of all DC subsets, which manifests as a major hematopoietic abnormality in young $Flt3^{ITD/+}$ animals. The cell-intrinsic effect of Flt3-ITD on DCs was accompanied by a cell-extrinsic effect on T cell homeostasis, including the expansion of T reg cells and dampened graft-versus-host responses. We propose that the newly described effect of Flt3-ITD might contribute to its leukemogenic capacity, e.g., by creating a DC-mediated tolerogenic environment and impairing immune surveillance by T cells.

RESULTS

DC lineage expansion in $Flt3^{ITD}$ animals

Heterozygous $Flt3^{ITD/+}$ mice are healthy and have normal hematopoiesis, whereas homozygous $Flt3^{ITD/ITD}$ mice display prominent myeloproliferation but only rare overt leukemia (Lee et al., 2007). As expected, young adult (5–14-wk-old) $Flt3^{ITD/+}$ mice contained normal fractions and numbers of major hematopoietic cell types, with only a slight (greater than twofold) increase in monocytes in the BM only (unpublished data). On the other hand, cDCs were significantly expanded several-fold in all lymphoid organs, including the BM, spleen, LNs, and thymus (Fig. 1, A and B). The cDC populations in nonlymphoid tissues, such as the small intestine, showed a similar expansion (unpublished data). pDCs were also significantly expanded in all organs except the thymus (Fig. 1, C and D). Homozygous $Flt3^{ITD/ITD}$ mice showed an even greater increase in all DC populations (Fig. 1, A–D), although other defects such as myeloproliferation and impaired B cell development were also observed as expected (unpublished data). Overall, DC expansion represented the most prominent hematopoietic phenotype in the heterozygous $Flt3^{ITD/+}$ mice (Fig. 1 E).

To analyze early DC development, we generated $Flt3^{ITD/+}$ mice carrying the Cx_3cr1^{GFP} reporter allele that has been widely used to visualize early DC progenitors (Geissmann et al., 2010). DC progenitors in the resulting Cx_3cr1^{GFP} animals were defined as shown in Fig. S1. Whereas the earliest progenitors of monocytes and DCs (macrophage/DC progenitors) were not increased significantly, CDPs and preDCs were expanded in absolute numbers (Fig. 1 F). In contrast, Cx_3cr1^{GFP}-negative progenitors, including the HSC population and erythromyeloid progenitors were unaffected (Fig. S1). We conclude that the specific DC expansion in $Flt3^{ITD/+}$ mice commences at the stage of Flt3-expressing common DC progenitors.

Expansion of DC populations is cell intrinsic

To test whether the effect of Flt3-ITD on DCs is cell intrinsic, we generated competitive BM chimeras and tracked the donor contribution with the CD45 congenic marker. Irradiated recipients ($CD45.1^+/CD45.2^+$) were injected with a 1:1 mixture of BM cells from wild-type mice ($CD45.1^+$) and either $Flt3^{+/+}$, $Flt3^{ITD/+}$, or $Flt3^{ITD/ITD}$ donor ($CD45.2^+$) mice. 14 wk after transfer, the fractions of cDCs from $Flt3^{ITD/+}$ and $Flt3^{ITD/ITD}$ donors were expanded, whereas wild-type $CD45.1^+$ competitor DCs were unaffected or reduced (Fig. 2, A and B). Similarly, the fraction of $Flt3^{ITD/+}$ donor-derived pDCs was significantly expanded (Fig. 2 C). The fraction of pDCs derived from $Flt3^{ITD/ITD}$ donors was not increased in the BM or spleen, likely caused by the expansion of other lineages in these organs. Similar trends were observed with absolute numbers of cDCs and pDCs (unpublished data).

The analysis of DC progenitor populations in recipient mice revealed the prominent expansion of CDPs and preDCs derived from $Flt3^{ITD/+}$ donor BM (Fig. 2 D). Although the analysis of DC progenitors derived from $Flt3^{ITD/ITD}$ donor BM was confounded by the absence of surface Flt3 (see below), an alternative gating strategy revealed a donor-specific expansion of $Flt3^{ITD/ITD}$ CDPs (Fig. S2). Thus, the Flt3-ITD mutation confers a cell-intrinsic competitive advantage to mature DCs and their progenitors.

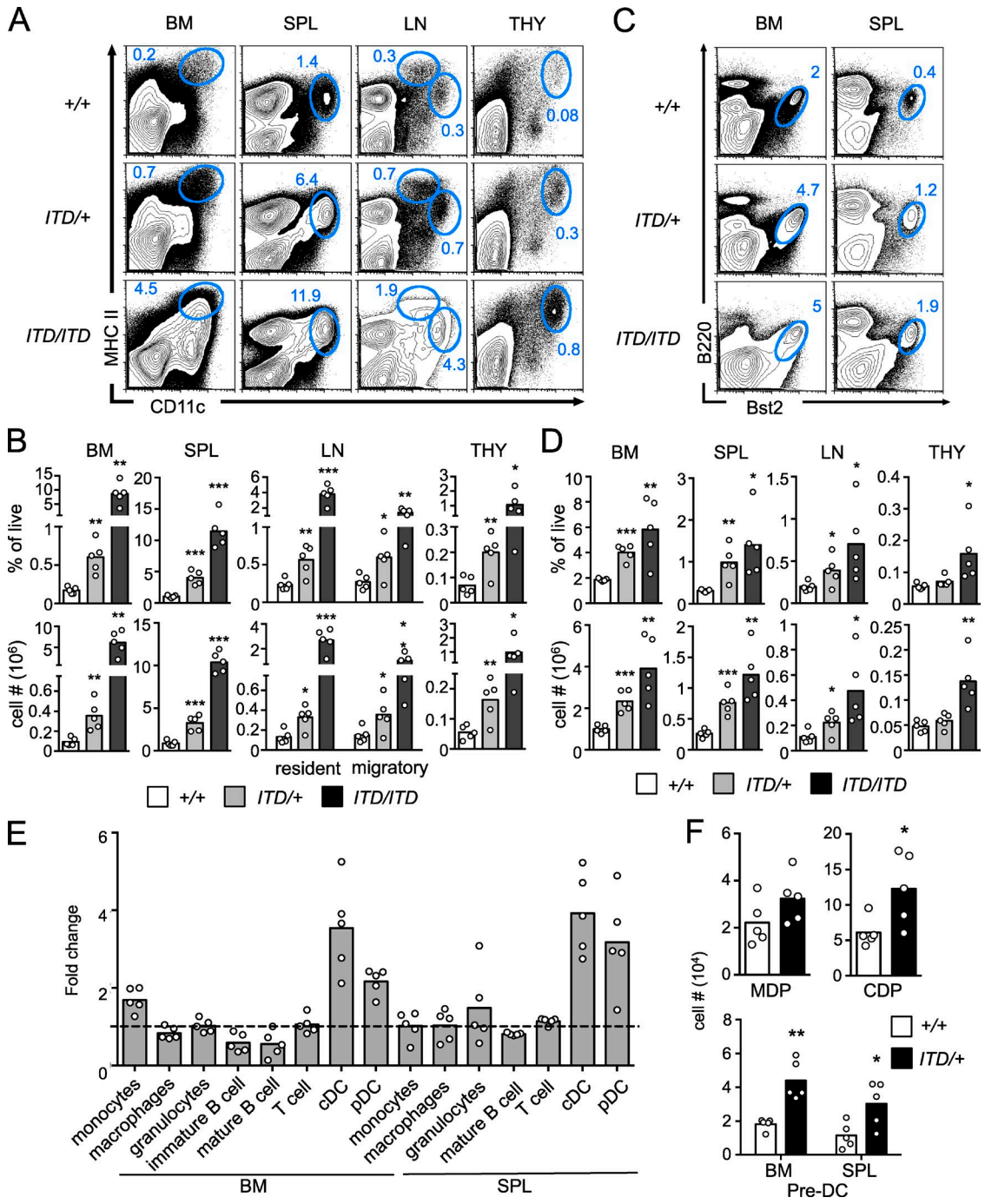

Figure 1. **Specific expansion of DC populations in Flt3-ITD mice.** (A–E) Adult B6 mice that were heterozygous (ITD/+) or homozygous (ITD/ITD) for the *Flt3*^{ITD} allele or wild-type (+/+) littermates were analyzed by flow cytometry for DC populations in the BM, spleen (SPL), LN, or thymus (THY). Bars indicate mean values of individual mice (circles) analyzed in five independent experiments (four in F). *, $P < 0.05$; **, $P < 0.01$; ***, $P < 0.001$, using unpaired, two-tailed Student's *t* test. (A) Representative staining plots with the fraction of CD11c^{hi} MHCII^{+} cDCs indicated. In the LN, CD11c^{hi} MHCII^{+} and CD11c^{lo} MHCII^{hi} populations represent resident and migratory cDCs, respectively. (B) Frequencies out of total live cells and absolute numbers of cDCs (mean, $n = 5$). (C) Representative staining plots with the fraction of B220^{+} Bst2^{+} pDCs indicated. (D) Frequencies and absolute numbers of pDCs (mean, $n = 5$). (E) Fold difference in the frequency of the indicated cell types between *Flt3*$^{ITD/+}$ and *Flt3*$^{+/+}$ mice. Frequencies from individual *Flt3*$^{ITD/+}$ mice were divided by a mean frequency of the corresponding cell type in *Flt3*$^{+/+}$ mice to derive mean fold difference ($n = 5$). (F) Heterozygous *Flt3*$^{ITD/+}$ (ITD/+) mice and wild-type B6 littermates (+/+) carrying the *Cx*$_3$*cr1*^{GFP} reporter allele were analyzed for DC progenitor populations as described in Fig. S1. Shown are the numbers of the indicated progenitors in the BM (mean, $n = 5$).

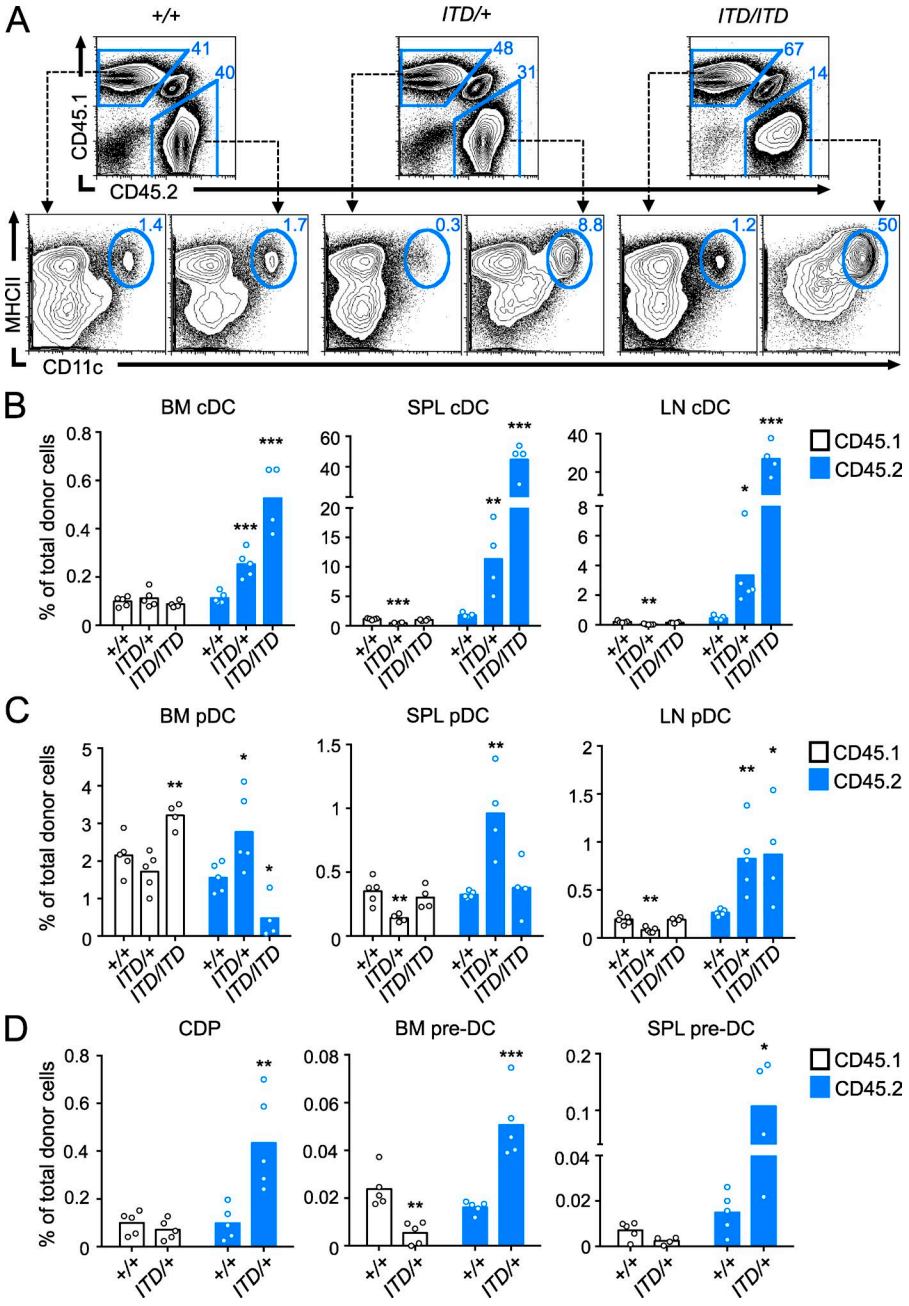

Figure 2. **Flt3-ITD expands DCs and DC progenitors in a cell-intrinsic manner.** Irradiated B6 × 129 F_1 recipients (CD45.1$^+$/CD45.2$^+$) were reconstituted with a 1:1 mixture of B6 CD45.1$^+$ wild-type competitor and B6 CD45.2$^+$ *Flt3*$^{+/+}$, *Flt3*$^{ITD/+}$, or *Flt3*$^{ITD/ITD}$ donor BM cells, and analyzed 14 wk later. Bars indicate mean values of four to five individual recipient mice (circles) in one reconstitution cohort; representative of two independent experiments. *, $P < 0.05$; **, $P < 0.01$; ***, $P < 0.001$, using unpaired, two-tailed Student's *t* test. (A) Representative staining plots of total splenocytes, showing donor-derived (CD45.1$^-$ CD45.2$^+$) and competitor-derived (CD45.1$^+$ CD45.2$^-$) populations and the cDC fraction within each of them. (B–D) The fraction of cDCs (B), pDCs (C), and DC progenitors (D) out of the total competitor-derived CD45.1$^+$ CD45.2$^-$ cells (open bars) or donor-derived CD45.1$^-$ CD45.2$^+$ cells (blue bars) in the BM, spleen (SPL), and LN (mean, n = 4–5). pDCs were defined as B220$^+$ CD11c^{lo} MHCII$^{lo/-}$ CD11b$^-$; CDPs as Lin$^-$ Sca-1$^-$ c-Kit^{lo} Flt3$^+$ CD115$^+$; and preDCs as Lin$^-$ (B220, CD3, NK1.1, CD11b, Gr-1, and Ter119) CD11c$^+$ MHCII$^-$ Flt3$^+$ Sirpα^-.

Flt3^{ITD} down-regulates surface Flt3 expression and abrogates Flt3L signaling in DCs

Myeloproliferation in *Flt3*$^{ITD/ITD}$ mice is accompanied by the loss of surface Flt3 expression and was proposed to occur independently of Flt3L (Kharazi et al., 2011). However, a role of exogenous Flt3L in leukemogenesis caused by Flt3-ITD has been demonstrated (Zheng et al., 2011; Bailey et al., 2013). We therefore examined the effect of Flt3-ITD on Flt3 expression and Flt3L signaling in the DC lineage. In the aforementioned competitive chimeras, Flt3 expression was significantly down-regulated in *Flt3*$^{ITD/ITD}$ donor-derived cDCs and pDCs but not in the corresponding wild-type cells (Fig. 3, A and B). A similar trend toward the down-regulation was observed in *Flt3*$^{ITD/+}$ donor-derived cells, although it reached significance only in pDCs. Moreover, CDPs from *Flt3*$^{ITD/+}$ and *Flt3*$^{ITD/ITD}$ donor BM showed a progressive reduction of surface Flt3 (Fig. 3, C and D).

To test how the observed down-regulation of Flt3 expression affects Flt3L-induced DC development, we cultured whole BM cells from *Flt3*$^{+/+}$, *Flt3*$^{ITD/+}$, and *Flt3*$^{ITD/ITD}$ mice with increasing concentrations of Flt3L. *Flt3*$^{ITD/+}$ BM showed a dose-dependent reduction of pDC development, whereas *Flt3*$^{ITD/ITD}$ BM was unable to generate cDCs or pDCs (Fig. 3 E). These data suggest that Flt3-ITD down-regulates

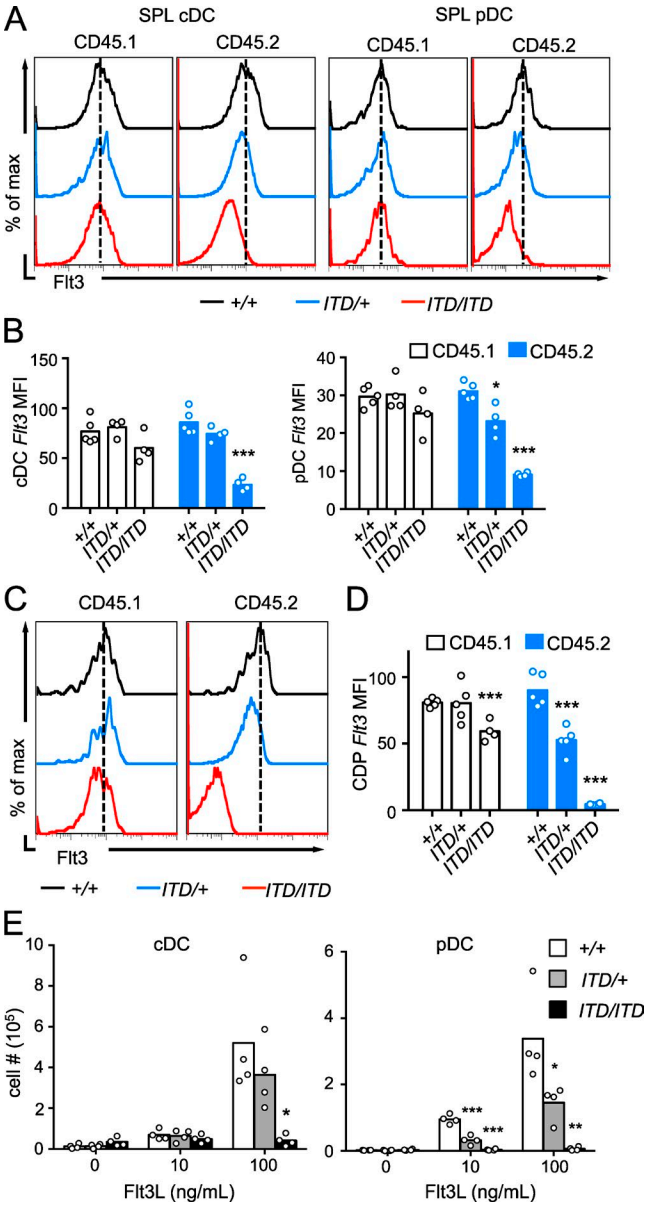

Figure 3. **Flt3-ITD causes down-regulation of surface Flt3 and abrogates Flt3L signaling.** (A) Representative histograms of Flt3 expression on the splenic cDCs and pDCs within the wild-type CD45.1$^+$ competitor and CD45.2$^+$ donor cells in the recipients described in Fig. 2. Dotted line shows mean fluorescence intensity (MFI) of Flt3 expression in cells derived from *Flt3*$^{+/+}$ donor. (B) The mean fluorescence intensity of Flt3 expression on competitor and donor splenic cDCs (left) and pDCs (right), as described in Fig. 2 (mean, $n = 4$–5). (C) Representative histograms of Flt3 expression on the CDPs in the BM of chimeric mice, shown as in panel A. CDPs were defined as Lin$^-$ Sca-1$^-$ IL7R$^-$ c-Kit^{lo} CD115$^+$. (D) The mean fluorescence intensity of Flt3 expression on competitor and donor BM CDPs, shown as in B. (E) Total BM cells from B6 *Flt3*$^{+/+}$, *Flt3*$^{ITD/+}$, or *Flt3*$^{ITD/ITD}$ littermates were cultured with the indicated concentrations of Flt3L, and the numbers of cDCs (CD11c$^+$ MHCII$^+$) and pDCs (B220$^+$ Bst2$^+$ CD11b$^-$) were determined by flow cytometry 7 d later. Bars indicate mean cell counts from four independent experiments (circles). *, $P < 0.05$; **, $P < 0.01$; ***, $P < 0.001$, using unpaired, two-tailed Student's *t* test.

Flt3 surface expression on DCs and renders them insensitive to exogenous Flt3L signaling. This appears to be detrimental in vitro, where the emergence and differentiation of DC progenitors are driven solely by Flt3L. In contrast, it appears to be compatible with DC development in vivo, where DC progenitors may be supported by other cytokines and Flt3 is partially redundant (Waskow et al., 2008; Ginhoux et al., 2009).

Flt3-ITD preferentially expands a noncanonical CD8$^+$ cDC subset

Mature cDCs in lymphoid organs comprise several genetically and functionally distinct subsets that can be identified using the *Cx$_3$cr1*^{GFP} reporter strain (Bar-On et al., 2010; Lewis et al., 2011). These include GFP^{lo} Esam^{hi} CD11b$^+$ cDCs that are efficient at CD4$^+$ T cell priming; GFP^{hi} Esam^{lo} CD11b$^+$ cDCs that preferentially produce cytokines; canonical GFP$^-$ CD8$^+$ cross-presenting cDCs; and noncanonical GFP^{hi} CD8$^+$ cDCs (nc-CD8$^+$) of unknown function. We analyzed the effect of Flt3-ITD on the subsets of cDCs using *Flt3*$^{+/+}$ or *Flt3*$^{ITD/+}$ mice carrying the *Cx$_3$cr1*^{GFP} reporter (Fig. 4 A). Although all four cDC subsets were significantly expanded, the GFP^{hi} nc-CD8$^+$ cDCs were particularly increased (Fig. 4, B and C). In contrast, Flt3L administration highly and preferentially expanded the canonical GFP$^-$ CD8$^+$ cDC subset (Fig. 4 C), as reported previously (Bar-On et al., 2010). Thus, Flt3-ITD causes a unique pattern of DC subset expansion that is distinct from exogenous Flt3L and favors the nc-CD8$^+$ cDCs.

Global gene expression analysis (Bar-On et al., 2010; and this study) suggested that nc-CD8$^+$ cDCs preferentially express PD-L1, a ligand of the inhibitory receptor PD-1 expressed on T cells. In combination with CD86 or Dec205, which are expressed on the canonical CD8$^+$ cDCs, PD-L1 identified the nc-CD8$^+$ cDC subset independent of *Cx$_3$cr1*^{GFP} (Fig. 4 D and not depicted). Indeed, the PD-L1$^+$ nc-CD8$^+$ cDCs were preferentially expanded in *Flt3*$^{ITD/+}$ mice (Fig. 4 E). To confirm this notion, we crossed *Flt3*$^{ITD/+}$ mice with Batf3-deficient mice that lack the canonical CD8$^+$ cDCs (Hildner et al., 2008; Bar-On et al., 2010). The resulting *Flt3*$^{ITD/+}$ *Batf3*$^{-/-}$ mice lacked the CD86$^+$ CD8$^+$ cDCs as expected, but showed the same prominent expansion of PD-L1$^+$ nc-CD8$^+$ cDCs (Fig. 4, F and G). The canonical Batf3-dependent cDCs are required for the establishment of infection by intracellular bacterium *Listeria monocytogenes* (*Lm*; Edelson et al., 2011), and their expansion facilitates the infection (Sathaliyawala et al., 2010). *Flt3*$^{ITD/+}$ mice showed a significant greater than twofold increase in *Lm* titers in the spleen (Fig. 4 H), consistent with the corresponding increase in canonical CD8$^+$ cDCs (Fig. 4, B and C). In contrast, *Flt3*$^{ITD/+}$ *Batf3*$^{-/-}$ mice were completely resistant to *Lm* infection, suggesting that the expanded nc-CD8$^+$ cDCs cannot substitute for the canonical CD8$^+$ cDCs (Fig. 4 H).

Characterization of *Flt3*$^{ITD/+}$ DCs

We analyzed the properties and expression profile of *Flt3*$^{ITD/+}$ DCs, including pDCs and the four cDC subsets (canonical

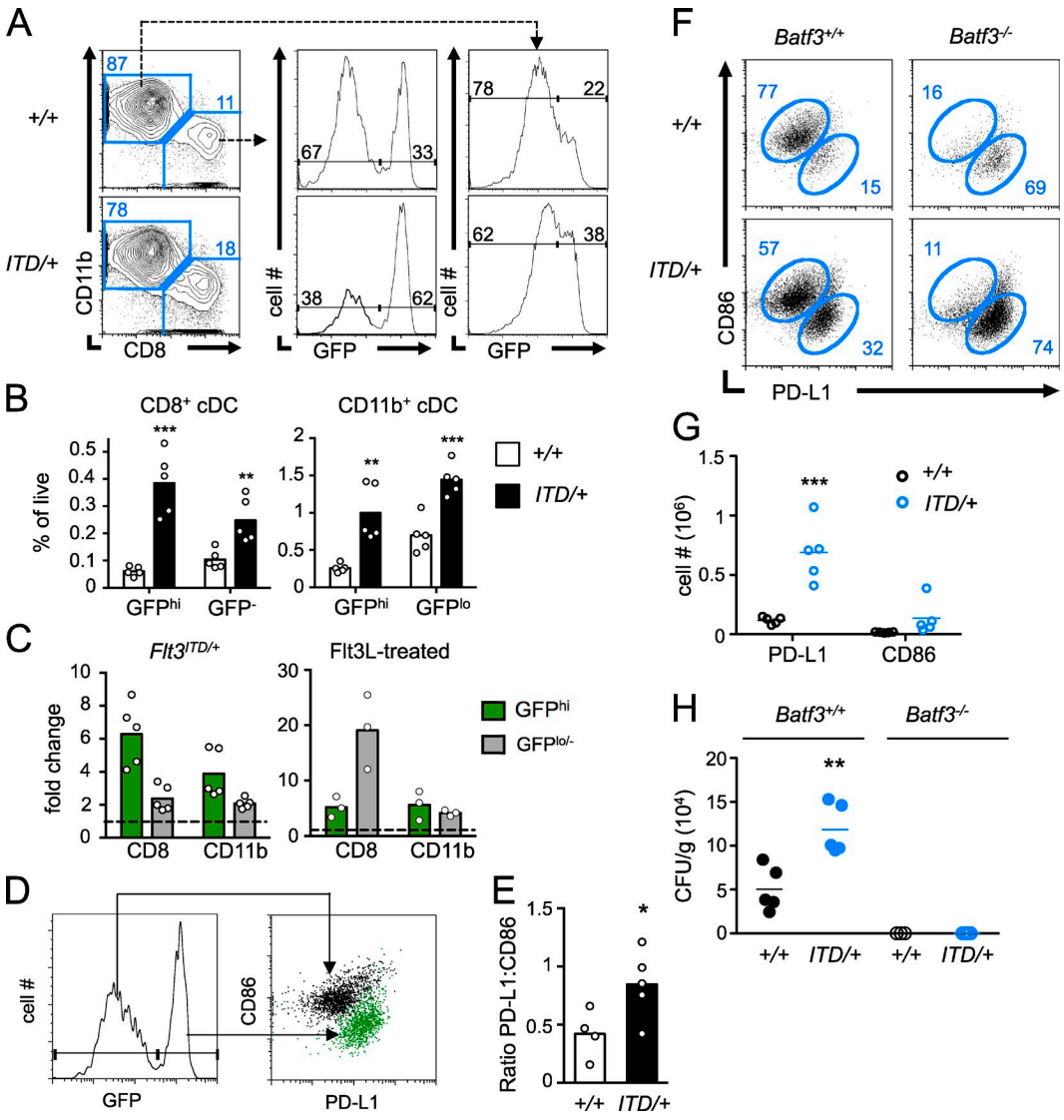

Figure 4. **Flt3-ITD promotes the expansion of a noncanonical CD8⁺ cDC subset.** (A) Representative staining plots of splenic CD11c^{hi} MHCII⁺ cDCs from *Cx$_3$cr1$^{GFP/+}$ Flt3$^{+/+}$* or *Flt3$^{ITD/+}$* mice, and the expression of GFP within the CD11b⁺ and CD8⁺ cDC populations. The levels of GFP used to define the subsets of CD8⁺ and CD11b⁺ cDCs are indicated. (B) The frequency of cDC subsets defined as in A within the spleens of B6 *Cx$_3$cr1$^{GFP/+}$ Flt3$^{+/+}$* and *Cx$_3$cr1$^{GFP/+}$ Flt3$^{ITD/+}$* littermates (mean, $n = 5$). Bars indicate mean values of individual mice per genotype (circles) analyzed in four independent experiments. (C) The fold-change cDC subsets in *Cx$_3$cr1$^{GFP/+}$* mice that either carry *Flt3$^{ITD/+}$* allele or were injected with recombinant Flt3L. The frequencies of each subset among total splenocytes in *Cx$_3$cr1$^{GFP/+}$ Flt3$^{ITD/+}$* mice were divided by the corresponding mean frequency in *Cx$_3$cr1$^{GFP/+}$ Flt3$^{+/+}$* littermates (left). The frequencies of each subset in *Cx$_3$cr1$^{GFP/+}$* mice injected with Flt3L were divided by the corresponding mean frequency in PBS-injected mice (right). Data represent mean frequency for five B6 *Cx$_3$cr1$^{GFP/+}$ Flt3$^{ITD/+}$* littermates analyzed from four independent experiments, and three B6 Flt3L-injected *Cx$_3$cr1$^{GFP/GFP}$* littermates representative of two independent experiments. (D) Representative analysis of CD86 and PD-L1 expression on the canonical and noncanonical CD8⁺ cDCs. Shown is the plot of CD86 versus PD-L1 expression on gated GFP^{hi} (green) and GFP^{lo} (black) splenic CD8⁺ cDCs from B6 *Cx$_3$cr1$^{GFP/GFP}$* mice. (E) The ratio of noncanonical PD-L1⁺ to canonical CD86⁺ subsets among splenic CD8⁺ cDCs from naive B6 *Flt3$^{+/+}$* or *Flt3$^{ITD/+}$* mice. Bars indicate mean values of four to five mice per genotype (circles), analyzed in two independent experiments. (F) Representative staining plots of gated splenic CD8⁺ cDC from wild-type or Batf3-deficient *Flt3$^{+/+}$* or *Flt3$^{ITD/+}$* mice. The canonical Batf3-dependent CD86⁺ subset and noncanonical PD-L1⁺ subset are indicated. (G) Fractions of CD8⁺ cDC subsets defined above in individual Batf3-deficient *Flt3$^{+/+}$* or *Flt3$^{ITD/+}$* mice. Values represent mean percentage from 5 individual mice pooled from two independent experiments. (H) Wild-type or Batf3-deficient B6 *Flt3$^{+/+}$* or *Flt3$^{ITD/+}$* mice were infected with *Lm* and sacrificed 3 d later. Shown are bacterial titers as colony-forming units per gram of spleen in individual mice of the indicated genotypes (mean, $n = 3–5$ per group). Representative of two independent experiments. Littermates of *Flt3$^{+/+}$* and *Flt3$^{ITD/+}$* within *Batf3$^{+/+}$* and *Batf3$^{-/-}$* crosses were pooled from different litters. *, $P < 0.05$; **, $P < 0.01$; ***, $P < 0.001$, using unpaired, two-tailed Student's *t* test.

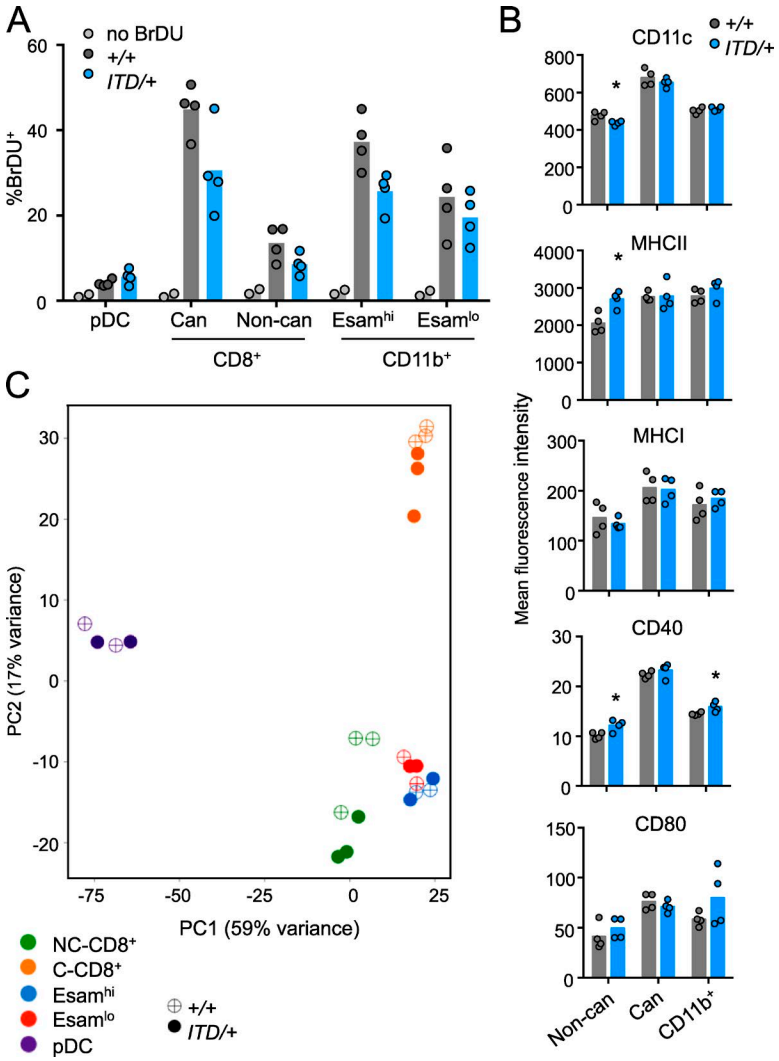

Figure 5. ***Flt3$^{ITD/+}$* DCs show normal proliferation rate and expression profile.** (A) *Flt3$^{ITD/+}$* mice or *Flt3$^{+/+}$* controls from an independent cross were administered BrdU for 2 d, and splenic DCs were analyzed for BrdU incorporation. Shown are percentages of BrdU incorporation within each DC subset. Canonical and noncanonical CD8$^+$ DCs were distinguished by Dec205 expression. Bars indicate mean values of two to four individual mice (circles) per genotype; representative of two independent experiments. Significance was calculated using unpaired, two-tailed Student's *t* test. (B) Mean fluorescence intensity of the indicated surface markers in cDC subsets, shown as in A. *, $P < 0.05$, using unpaired, two-tailed Student's *t* test. (C) Principal component analysis of global RNA-Seq expression profiles of sorted splenic DC populations from *Flt3$^{+/+}$* or *Flt3$^{ITD/+}$* mice. Symbols represents individual RNA-Seq profiles of each population sorted in an independent experiment (three biological replicates for each CD8$^+$ cDC subset, two for each CD11b$^+$ cDC subset, and two for pDCs, from four independent experiments).

CD8$^+$, nc-CD8$^+$, CD11b$^+$ Esam^{hi}, and CD11b$^+$ Esam^{lo}). All *Flt3$^{ITD/+}$* DCs showed normal incorporation of BrdU during a 2-d pulse, revealing that their proliferation was unchanged (Fig. 5 A). Together with increased CDP numbers (Fig. 1 F) and enhanced DC production by *Flt3$^{ITD/+}$* myeloid progenitors in vitro (unpublished data), this suggests that DC expansion in *Flt3$^{ITD/+}$* mice occurs at the level of progenitors rather than mature DCs. Similarly, surface expression of MHC proteins and co-stimulatory molecules such as CD80 and CD40 was normal on all *Flt3$^{ITD/+}$* cDCs (Fig. 5 B). Next, we characterized global gene expression profiles of the five DC subsets from wild-type and *Flt3$^{ITD/+}$* mice by RNA sequencing (RNA-Seq). Wild-type DC subsets showed the expected differential expression of signature markers and transcription factors (Fig. 6 A). Principal component analysis (Fig. 5 C) confirmed that pDCs, canonical CD8$^+$ cDCs, and CD11b$^+$ cDCs (both subsets) have distinct expression profiles, whereas nc-CD8$^+$ resemble CD11b$^+$ cDCs and pDCs (Bar-On et al., 2010). All *Flt3$^{ITD/+}$* DC subsets clustered closely with their wild-type counterparts, suggesting that their expression profiles were largely preserved.

Given the dominant nature of the Flt3-ITD mutation, we focused specifically on the genes induced in *Flt3$^{ITD/+}$* DCs. Several genes were induced in multiple DC subsets, including *Cdh2* and *Socs2*, a negative feedback regulator of cytokine signaling and a common target of Flt3-ITD in AML (Sen et al., 2012; Fig. 6 B and supplemental dataset). Pairwise comparison of expression profiles showed that canonical CD8$^+$ cDCs and nc-CD8$^+$ cDCs harbored the largest number of induced genes (Fig. 6 B). Although most of the genes were induced only modestly, we noticed the induction of several genes associated with immunological tolerance and/or T reg cell function in both CD8$^+$ cDC subsets (Fig. 6, C and D). These included amphiregulin (*Areg*; Zaiss et al., 2015), adrenomedullin (*Adm*; Rullé et al., 2012), Cox-2 (*Ptgs2*; Zelenay et al., 2015), and adenosine 2A receptor (*Adora2a*; Li et al., 2012). We conclude that *Flt3$^{ITD/+}$* DCs have largely normal phenotypes and

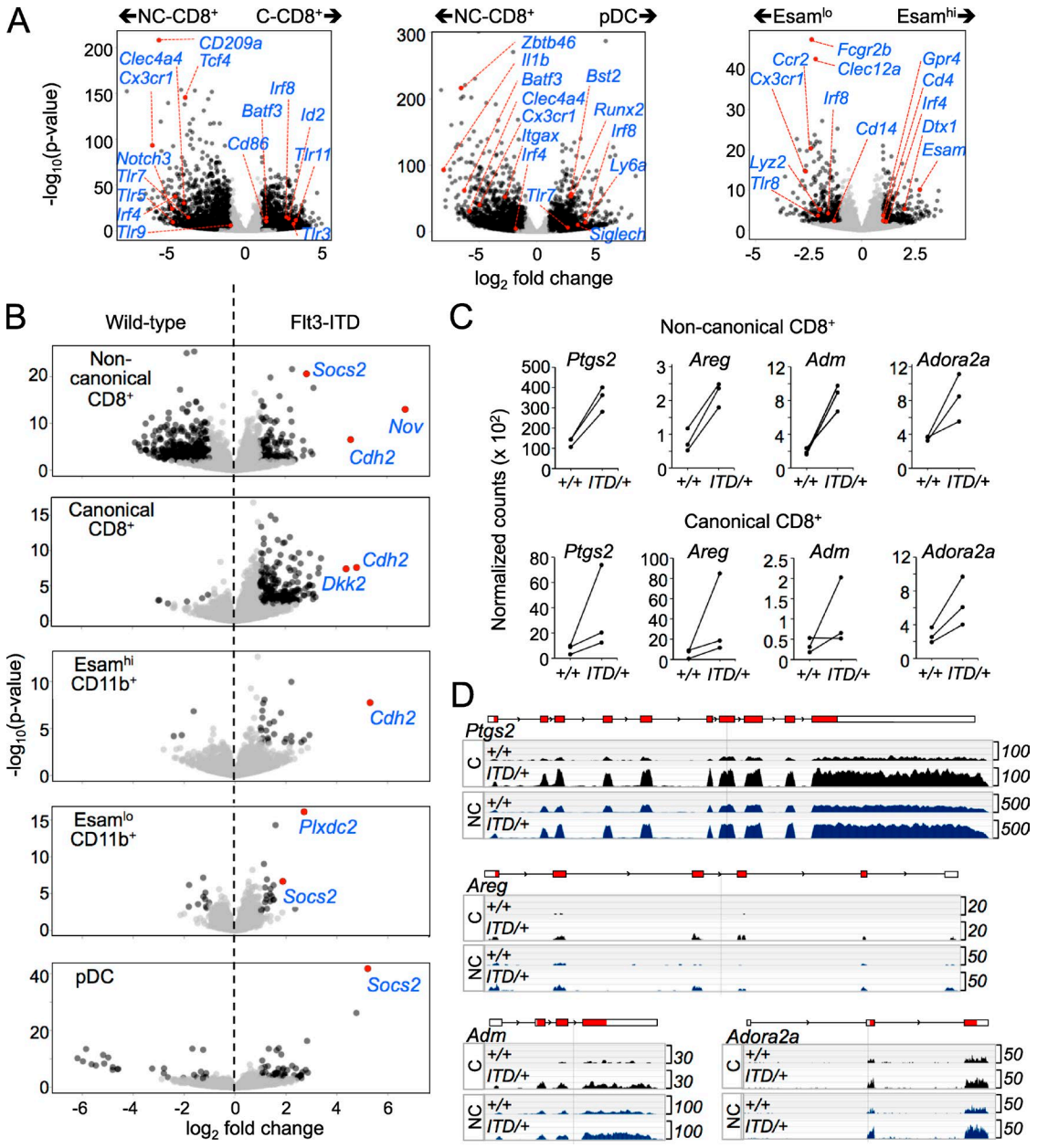

Figure 6. **Flt3-ITD preferentially affects gene expression in CD8⁺ cDCs.** (A–D) Splenic DC subsets isolated from *Flt3*$^{+/+}$ or *Flt3*$^{ITD/+}$ littermates were analyzed by RNA-Seq (three biological replicates for each CD8⁺ cDC subset, two for each CD11b⁺ cDC subset, and two for pDCs, from four independent experiments). (A and B) Pairwise comparison of averaged individual gene signals comparing indicated DC subsets from *Flt3*$^{+/+}$ mice (A) or comparing *Flt3*$^{+/+}$ and *Flt3*$^{ITD/+}$ mice within indicated DC subsets (B). Genes were plotted by moderated $\log_2$ fold change against $-\log_{10}$ of the statistical p-values (Wald test); black points represent genes with $\log_2$ fold change ≥1, adjusted p-values <0.1, and statistical p-values <0.05. Several prominently up-regulated genes are highlighted in red. Note that the abundantly overexpressed genes in wild-type noncanonical CD8⁺ cDCs reflect contamination with non-DC in two replicates. (C) Normalized read counts of *Ptgs2*, *Areg*, *Adm*, and *Adora2a* in paired biological replicates of CD8⁺ cDC subsets. (D) Representative raw counts mapped to gene loci of *Ptgs2*, *Areg*, *Adm*, and *Adora2a* within CD8⁺ cDCs.

gene expression, with the few induced changes in canonical CD8⁺ cDCs and nc-CD8⁺ cDCs consistent with a tolerogenic function.

Flt3$^{ITD/+}$ expands T cells in a cell-extrinsic manner

Given the important role of DCs in T cell homeostasis and especially in T reg cell maintenance, we examined T cell pop-

ulations in Flt3-ITD–carrying mice. No significant differences in the numbers of conventional T (T conv) cells were observed in the BM, spleens, or LNs of these mice (Fig. 7 A). However, the fraction and absolute numbers of $CD4^+$ $FoxP3^+$ T reg cells were progressively increased in the BM of $Flt3^{ITD/+}$ and $Flt3^{ITD/ITD}$ mice (Fig. 7 B). To test whether the observed effects on T cells were cell intrinsic, we examined T cell populations in the competitive chimeras described in the legend to Fig. 2. Donor-derived T conv and T reg cell populations were unchanged for $Flt3^{ITD/+}$ donors and markedly reduced for $Flt3^{ITD/ITD}$ donors, consistent with impaired lymphopoiesis in the latter (Fig. 7, C and D). In contrast, the fraction of wild-type T conv cells in the recipients of $Flt3^{ITD/+}$ cells was significantly increased in the BM and, to a lesser extent, in the spleen (Fig. 7 C). Moreover, wild-type T reg cells were also expanded in the BM, spleen, and LN (Fig. 7 D), causing a significant increase in the T reg cell fraction out of total T cells (Fig. 7 E). No increases of competitor T cells were observed in the recipients of $Flt3^{ITD/ITD}$ cells, likely reflecting the profound decrease of donor-derived T cells. We conclude that heterozygous Flt3-ITD mutation causes a cell-extrinsic expansion of T cells that favors the T reg cell population.

Flt3-ITD–expressing DCs facilitate antigen-driven and homeostatic T cell proliferation

Given the cell-intrinsic effect of Flt3-ITD on DCs, we hypothesized that these cells may mediate the cell-extrinsic effect of the mutation on T cells. To test this notion, we set up allogeneic mixed leukocyte reactions (MLRs) with $Flt3^{ITD/+}$ splenic DCs as stimulators and wild-type T cells as responders. To differentiate conventional and regulatory T cell populations, we used T cells from the $FoxP3^{GFP}$ reporter mice in which T reg cells express GFP. Compared with control $Flt3^{+/+}$ DCs, similar numbers of $Flt3^{ITD/+}$ DCs induced greater expansion of allogeneic $CD4^+$ T conv, $CD8^+$ T conv, and T reg cells (Fig. 8 A). Notably, the fraction of T reg cells among total responder T cells was significantly increased as a result (Fig. 8 B). Accordingly, all T cell populations stimulated with $Flt3^{ITD/+}$ DCs showed more extensive proliferation as measured by the dilution of the tracer dye Cell Trace Violet (CTV; Fig. 8 C). Isolated cDC subsets also stimulated T cell proliferation but did not yield increased T reg cell proportions (unpublished data), suggesting that the latter may require cross talk between several subsets.

To further dissect the cell-extrinsic effect of Flt3-ITD on T cells in vivo, we generated $Flt3^{ITD/+}$ Rag1-deficient mice that lack endogenous T or B cells. The transfer of wild-type T cells into lymphopenic mice causes a rapid T cell expansion that depends on microbiota-derived antigens, and a slower cytokine-driven homeostatic proliferation (Takada and Jameson, 2009). We transferred CTV-labeled wild-type T cells from $FoxP3^{GFP}$ mice into control $Flt3^{+/+}$ $Rag1^{-/-}$ or $Flt3^{ITD/+}$ $Rag1^{-/-}$ mice. The resulting numbers of all T cell populations were significantly increased in $Flt3^{ITD/+}$ lymphopenic recipients (Fig. 8 D). The proportion of T cells that underwent homeostatic proliferation was not substantially changed (Fig. 8 E), suggesting that Flt3-ITD facilitates both the proliferation and survival of T cells in vivo in a cell-extrinsic manner.

$Flt3^{ITD/+}$ expands the T reg cell population and dampens alloreactive T cell responses

Consistent with the preferential expansion of T reg cells by Flt3L administration, they were also preferentially expanded in the presence of Flt3-ITD–expressing cells (Fig. 7 E and Fig. 8 B). To directly analyze T reg cell homeostasis in $Flt3^{ITD/+}$ mice, we used the $FoxP3^{DTR\text{-}GFP}$ strain that allows both the detection of T reg cells by GFP expression and their specific depletion by administration of diphtheria toxin (DT; Kim et al., 2007). The resulting sensitive detection of T reg cells in naive $Flt3^{ITD/+}$ $FoxP3^{DTR\text{-}GFP}$ mice revealed a greater proportion of T reg cells out of T cells in the spleen (Fig. 9 A), but not in the thymus or blood (Fig. 9, A and B). Upon DT-mediated depletion, $Flt3^{ITD/+}$ mice supported a more robust reconstitution of blood T reg cells at days 10–28 (Fig. 9 B). Although T conv cells also underwent compensatory expansion, the fraction of T reg cells among total T cells was significantly increased in $Flt3^{ITD/+}$ mice on day 21 (Fig. 9 B). At the 28 d endpoint, the fraction of T reg cells among T cells was significantly increased in the spleens and thymi of $Flt3^{ITD/+}$ mice (Fig. 9 A).

Flt3L-mediated T reg cell expansion has been associated with reduced alloreactive T cell response during acute experimental GVHD (Swee et al., 2009). To test whether Flt3-ITD has a similar tolerogenic effect, we transferred wild-type B6 lymphocytes ($CD45.2^+$) into nonirradiated (B6xFVB) F_1 hosts ($CD45.1^+/CD45.2^+$) that were $Flt3^{+/+}$ or $Flt3^{ITD/+}$. 1 wk later, the frequency and number of the transferred T cells were significantly reduced in $Flt3^{ITD/+}$ compared with $Flt3^{+/+}$ recipients (Fig. 9, C and D). This was accompanied by an increased fraction of T reg cells among host T cells (unpublished data). Given the expansion of PD-$L1^+$ $CD8^+$ cDCs (Fig. 4), we tested whether the reduced alloreactive response was dependent on the PD-L1–PD-1 pathway by treating recipients with anti–PD-L1 or anti-PD-1 antibodies. As expected (Blazar et al., 2003), PD-1 blockade led to a greater expansion of alloreactive T cells (Fig. 9 E). However, T cell expansion was still severely reduced in $Flt3^{ITD/+}$ compared with $Flt3^{+/+}$ recipients treated with either anti–PD-L1 or anti–PD-1, suggesting that the effect of Flt3-ITD is not solely dependent on this pathway.

Finally, we asked whether the dampening of T cell responses against self-antigens in $Flt3^{ITD/+}$ recipients is indeed dependent on T reg cells. To this end, we crossed $Flt3^{ITD/+}$ mice with $FoxP3^{sf}$ (scurfy) mice that lack functional T reg cells and develop lethal T cell–mediated autoimmunity. If Flt3-ITD directly impaired self-reactive effector T cell responses, one would expect that the autoimmunity in $Flt3^{ITD/+}$ $FoxP3^{sf}$ mice would be ameliorated. In contrast, we found that these mice died significantly sooner than $Flt3^{+/+}$ $FoxP3^{sf}$ littermates (Fig. 9 F). Collectively, these results suggest that Flt3-ITD mutation causes a preferential expansion

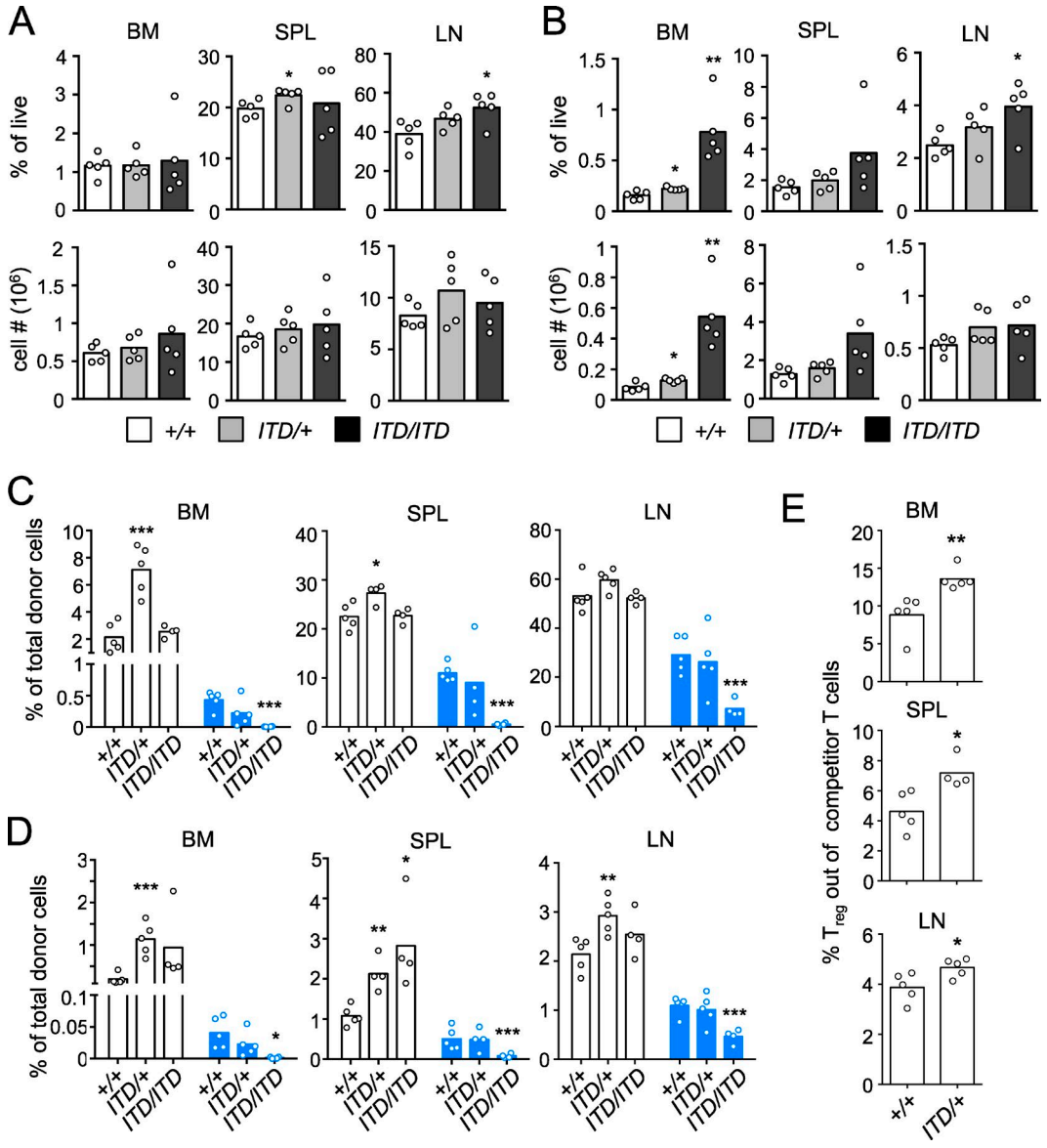

Figure 7. **Flt3-ITD expands T cell populations in a cell-extrinsic manner.** The populations of TCRβ+ FoxP3− conventional (T conv) and TCRβ+ CD4+ FoxP3+ regulatory (T reg) T cells were analyzed in the lymphoid organs by intracellular staining for FoxP3. *, $P < 0.05$; **, $P < 0.01$; ***, $P < 0.001$, using unpaired, two-tailed Student's *t* test. (A and B) The frequencies and absolute numbers of T conv cells (A) and T reg cells (B) cells in naive B6 *Flt3*$^{+/+}$, *Flt3*$^{ITD/+}$, or *Flt3*$^{ITD/ITD}$ littermates. Bars indicate mean values of five individual mice (circles) analyzed in five independent experiments. (C and D) The fraction of T conv cells (C) and T reg cells (D) cells out of the total competitor-derived CD45.1+ CD45.2− cells (open bars) or donor-derived CD45.1− CD45.2+ cells (blue bars) in the recipient mice described in Fig. 2. (E) The percentage of T reg cells out of total CD45.1+ competitor T cells in the recipients reconstituted with *Flt3*$^{+/+}$ or *Flt3*$^{ITD/+}$ donor cells as described in Fig. 2.

of T reg cells, which is accompanied by dampened T cell responses against self-antigens.

DISCUSSION

Constitutive activation of the growth factor receptor Flt3 represents the most common genetic abnormality in AML. Therefore, Flt3 signaling has been extensively studied in the context of leukemogenesis, where mutant variants such as Flt3-ITD are thought to promote the growth of Flt3-expressing transformed progenitors. Separately, Flt3 signaling is known as a critical regulator of DC development and homeostasis, and DC expansion represents the most striking consequence of Flt3 activation by the exogenous ligand. Here, we combined the two facets of Flt3 activation by testing the effect of Flt3-ITD on DC development and its immunological consequences.

We found that the endogenous Flt3-ITD caused an early cell-intrinsic expansion of all DC subsets and their

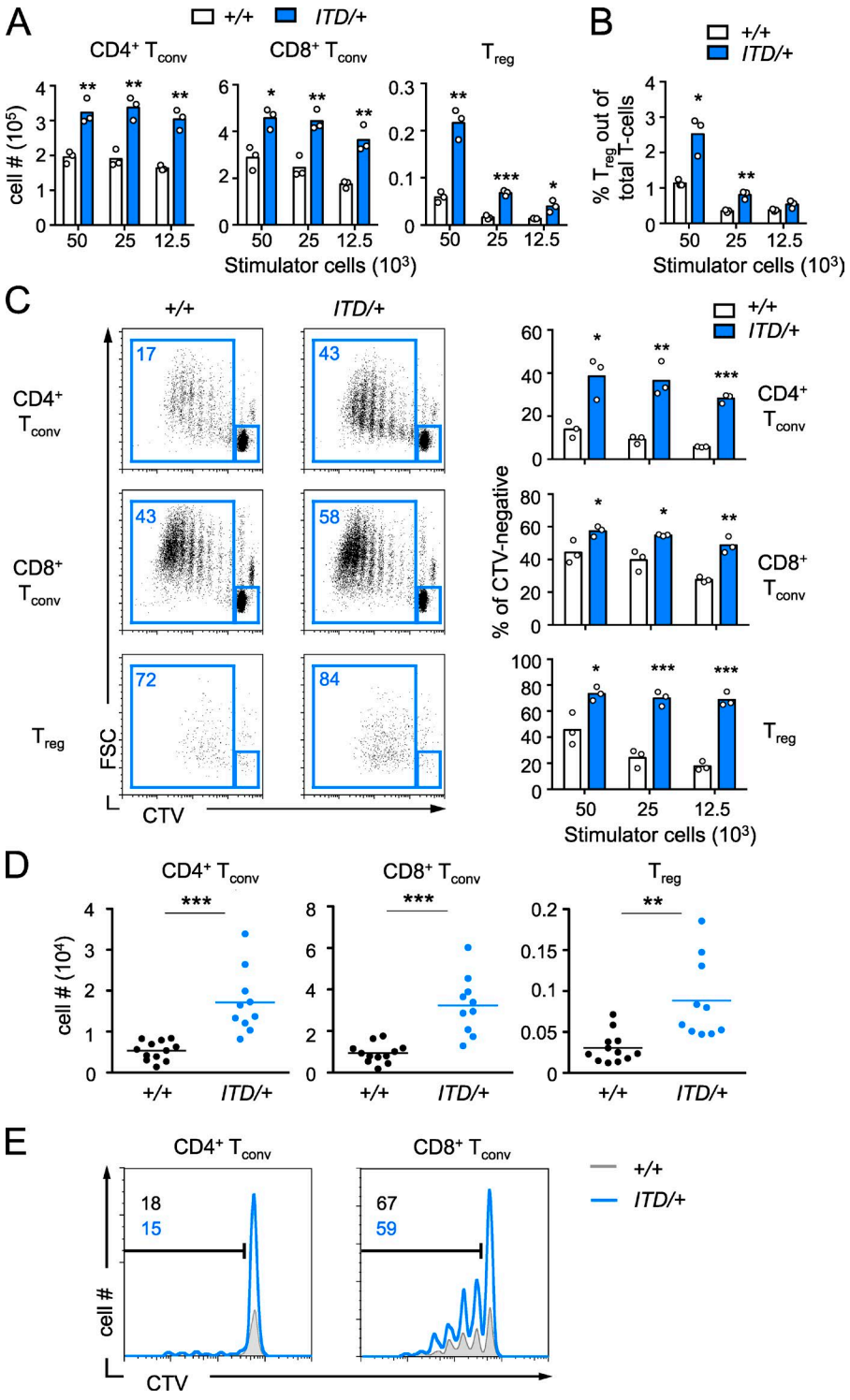

Figure 8. **Flt3-ITD facilitates antigen-driven and homeostatic T cell proliferation.** (A–C) MLRs were set up with CD11c$^+$ splenocytes from B6xFVB *Flt3*$^{+/+}$ or *Flt3*$^{ITD/+}$ littermates (n = 3 per genotype) as stimulators and CTV-labeled allogeneic T cells from B6 *FoxP3*^{GFP} mice as responders. The fractions of GFP$^-$ conventional (T conv) and GFP$^+$ regulatory (T reg) responder T cells were analyzed 4 d later. Bars indicate mean values of three biological replicates (circles); representative of three independent experiments. *, $P < 0.05$; **, $P < 0.01$; ***, $P < 0.001$, using unpaired, two-tailed Student's t test. (A) Absolute numbers of responder T cell populations from the MLRs above. (B) The proportion of responder T reg cells out of responder T cells from the MLRs above. (C) Representative staining profiles and fractions of proliferating responder T cells that have diluted the CTV dye in the MLRs above. (D and E) CTV-labeled lymphocytes from *FoxP3*^{GFP} mice were transferred into Rag1-deficient *Flt3*$^{+/+}$ or *Flt3*$^{ITD/+}$ mice. Adoptively transferred T cell populations were analyzed in the spleens of recipient animals 5 d later. (D) Numbers of GFP$^-$ conventional (T conv) and GFP$^+$ regulatory (T reg) T cells in 10–12 individual recipient mice (circles) per group and their averages (lines) pooled from two independent experiments. (E) Representative histograms of CTV dye levels in T conv cells, with the proportion of dye-diluting proliferative T cells indicated.

progenitors (CDP). Because CDP did not support enhanced DC development in vitro (unpublished data), the expansion is likely to originate in the earlier Flt3$^+$ progenitors, such as macrophage/DC or even HSC/multipotent progenitors. As in the case of myeloid progenitors (Kharazi et al., 2011), Flt3-ITD in DCs caused the loss of surface Flt3 expression and of the responsiveness to Flt3L, suggesting that its primary function is independent of Flt3L. The effect of Flt3-ITD on DCs was allele dosage-dependent and was highly significant even in heterozygous *Flt3*$^{ITD/+}$ mice that appear normal otherwise. Thus, DC lineage expansion represents a prominent consequence of the germ-line Flt3-ITD mu-

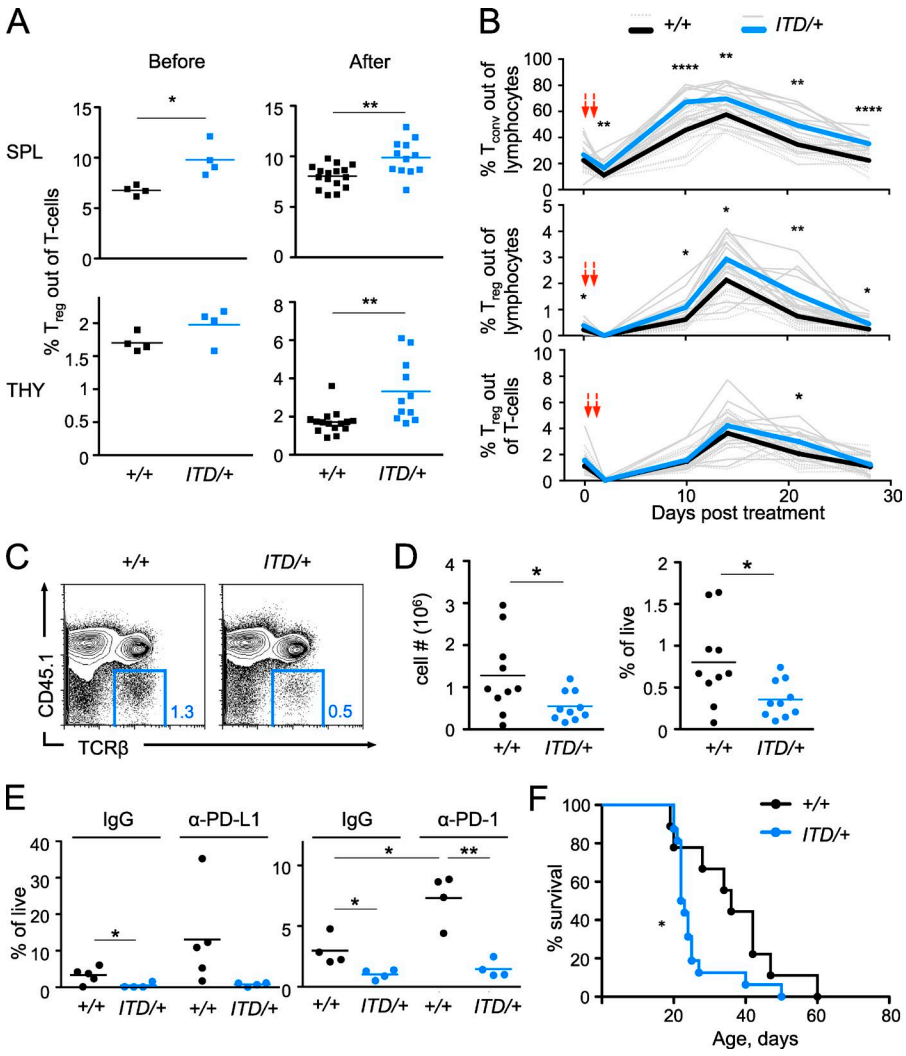

Figure 9. **Flt3-ITD favors T reg cell expansion and dampens self-reactivity in the presence of T reg cells.** (A and B) B6 *Flt3*$^{+/+}$ or *Flt3*$^{ITD/+}$ mice carrying the *Foxp3*$^{DTR\text{-}GFP}$ allele were treated with DT twice to deplete T reg cells, and the GFP^{+} T reg cell population was analyzed at different time points. Data represent four animals (before treatment) or 12–16 animals (after treatment) per genotype pooled from three independent experiments. In some of the experiments, nonlittermate wild-type mice derived from the same cross were used. *, $P < 0.05$; **, $P < 0.01$; ****, $P < 0.0001$, using unpaired, two-tailed Student's *t* test. (A) The frequency of T reg cell out of total T cells in the spleens and thymi of naive mice before treatment or of DT-treated mice 28 d after the treatment. (B) The frequency of T conv cell (top) and T reg cell (middle) out of total lymphocytes, and frequency of T reg cell out of total T cells (bottom) in the peripheral blood of mice before DT (day 0) or after DT administration (red arrows). Individual animals and group averages are shown as thin and thick lines, respectively. (C and D) Wild-type splenocytes and LN cells were transferred into semiallogeneic B6xFVB *Flt3*$^{+/+}$ or *Flt3*$^{ITD/+}$ littermates to induce graft-versus-host response. (C) Representative staining profile of total splenocytes from recipient mice 7 d after the transfer, with donor-derived CD45.1^{-} T cells highlighted. (D) Absolute numbers and frequencies of donor-derived T cells in the spleens of individual recipient mice (mean, $n = 10$). Representative of three independent experiments.(E) Frequencies of donor-derived T cells in the spleens of individual B6 *Flt3*$^{+/+}$ or *Flt3*$^{ITD/+}$ littermates that were treated with IgG control, anti-PD-L1 or anti-PD-1 blocking antibodies prior and during the transfer (mean, $n = 4–5$). Representative of two independent experiments each. (F) The survival of T reg cell–deficient B6 *FoxP3*^{sf}/*y* (Scurfy) mice that were *Flt3*$^{+/+}$ or *Flt3*$^{ITD/+}$ ($n = 9–16$). Mice are pooled from seven litters from the same cross. *, $P < 0.05$, using log-rank (Mantel-Cox) test.

tation in the steady state, thereby recapitulating the effects of Flt3L administration.

Exogenous Flt3L is known to expand DC subsets to various extents, particularly favoring the canonical cross-presenting CD8^{+} cDCs (O'Keeffe et al., 2002;Varol et al., 2009; Bar-On et al., 2010). The canonical CD8^{+} cDCs were expanded by only approximately twofold in *Flt3*$^{ITD/+}$ mice, along with the corresponding increase in bacterial titers upon *Listeria* infection as expected (Sathaliyawala et al., 2010). In contrast, the greatest expansion occurred in the noncanonical subset of CD8^{+} cDCs, which appear to be related to pDCs yet lack the cytokine-producing abilities of pDCs or canonical CD8^{+} cDCs (Bar-On

et al., 2010). Flt3L–Flt3 signaling in DCs is mediated primarily by Stat3 (Laouar et al., 2003) and by the PI(3)K–mTOR pathway (Sathaliyawala et al., 2010). However, Flt3-ITD activates multiple pathways, including PI(3)K, Stat5, and Ras–MAPK, and their relative balance likely differs from that of the normal receptor (Parcells et al., 2006). Therefore, our results suggest that genetic and pharmacological activation of Flt3 are similar but not identical, and may involve different downstream effectors. Importantly, both $CD8^+$ cDC subsets showed the largest effect of Flt3-ITD on gene expression and, notably, up-regulated a set of genes associated with tolerance.

The expansion of DCs by Flt3L administration has a complex indirect effect on T cells, both enhancing and inhibiting various T cell responses (Sela et al., 2011; Anandasabapathy et al., 2014). Importantly, it has been demonstrated to increase the number of T reg cells and facilitate their function both in mice (Darrasse-Jèze et al., 2009; Swee et al., 2009) and humans (Klein et al., 2013). The effects on T reg cells may be caused by the numerical expansion of DCs, as well as by modified functionality of Flt3L-expanded DCs on a per cell basis (Sela et al., 2011). As a result, Flt3L administration dampens T cell responses to self-antigens in the contexts of tissue inflammation and GVHD (Chilton et al., 2004; Darrasse-Jèze et al., 2009; Swee et al., 2009; Collins et al., 2012; Svensson et al., 2013). Similarly, we found that FLT3-ITD–expressing DCs more efficiently support T cell proliferation in vitro and in vivo, and particularly favor the expansion of T reg cells as confirmed in a model of specific T reg cell ablation. The observed T reg cell expansion was accompanied by reduced alloreactive T cell response during GVHD; in contrast, Flt3-ITD enhanced rather than dampened autoreactivity in the absence of T reg cells. These data suggest that FLT3-ITD resembles pharmacological Flt3 activation in creating a tolerogenic environment via a DC-mediated enhancement of T reg cell function. As such, they provide robust genetic evidence for the role of DCs in T reg cell homeostasis (Darrasse-Jèze et al., 2009; Swee et al., 2009; Bar-On et al., 2011).

Recent genome-wide analysis of human AML showed that *FLT3* mutation is a relatively late event in AML progression (Jan et al., 2012; Shlush et al., 2014). Nevertheless, it may occur sufficiently early so that the resulting FLT3-ITD mutation is transmitted to normal hematopoietic hierarchy. Critically, peripheral blood DCs in AML patients were shown to express the mutant FLT3-ITD receptor and manifest higher frequencies and functional abnormalities (Rickmann et al., 2011, 2013). Indeed, the short-lived DCs are constantly replenished (Liu et al., 2007), therefore they should quickly inherit any mutation from the stem/progenitor compartment. Furthermore, increased frequency of T reg cells has been demonstrated in AML, and its reduction by various therapeutic approaches represents a promising treatment strategy for the disease (Schick et al., 2013; Yang and Xu, 2013; Bachanova et al., 2014; Govindaraj et al., 2014). These emerging data suggest that, similar to the animal model described here, FLT3-ITD in human AML patients is expressed in the DC lineage and may cause its expansion, leading to enhanced T reg cell function.

In conclusion, our study documents a novel major effect of the leukemogenic Flt3 mutation on normal hematopoiesis, including the modulation of DC and T cell numbers and function. This effect appears to precede overt leukemogenesis and involve both cell-intrinsic and -extrinsic components. Together with the described impairment of HSC maintenance (Chu et al., 2012) and of lymphopoiesis (Mead et al., 2013), our results reveal a profound modulation of normal hematopoiesis by FLT3-ITD. It is tempting to speculate that the observed modulation of DC and T reg cell function might impair immunosurveillance, thereby facilitating the escape of the mutant leukemic clone. This scenario would become directly testable with the advent of experimental models of immunosurveillance in leukemia. In addition, the observed effects on GVHD may be relevant for graft-versus-leukemia response that eliminates residual leukemic cells after allogeneic BM transplantation. This hypothetical mechanism of immunoevasion would be unique to hematopoietic tumors, which originate from the same source as the immune system and therefore might subvert the latter through leukemogenic mutations.

MATERIALS AND METHODS

Animals. All animal studies were performed according to the investigator's protocol approved by the Institutional Animal Care and Use Committee of Columbia University and New York University Langone Medical Center. $Flt3^{ITD/+}$ (Lee et al., 2007), $CX3CR1^{GFP/GFP}$ (Jung et al., 2000), $Batf3^{-/-}$ (Hildner et al., 2008), $FoxP3^{DTR\text{-}GFP}$ (Kim et al., 2007), $FoxP3^{GFP}$ (Fontenot et al., 2005), $FoxP3^{Sf}$, and $Rag1^{-/-}$ mice were obtained from The Jackson Laboratory. All mice were on pure C57BL/6 (B6) background and were maintained by crossing to wild-type B6 mice. Unless indicated otherwise, $Flt3^{+/+}$ littermates of $Flt3^{ITD/+}$ or of $Flt3^{ITD/ITD}$ animals were used as wild-type controls. To study allogeneic T cell responses, $Flt3^{ITD/+}$ mice were crossed to FVB/N mice (Taconic) to generate wild-type of $Flt3^{ITD/+}$ (B6xFVB) F_1 littermates. For T reg cell depletion model, $FoxP3^{DTR\text{-}GFP/DTR\text{-}GFP}$ females were crossed to $Flt3^{ITD/+}$ males, and male progeny were studied. For T cell–mediated autoimmunity model, $FoxP3^{sf/+}$ females were bred to $Flt3^{ITD/+}$ males, and only male $FoxP3^{sf}$/y progeny were studied. Mice were analyzed at 5–14 wk of age unless otherwise noted.

DC preparation and culture. Lymphoid organs were digested with collagenase D (1 mg/ml) and DNase I (20 µg/ml) in DMEM/10% FCS for 30–60 min at 37°C before generating single-cell suspensions, and red blood cells were lysed. For Flt3L-driven DC development in vitro, total BM cells were plated in triplicates in a 24-well plate (2×10^6 per well) in DMEM/10% FCS with the indicated concentrations of recombinant murine Flt3L (PeproTech) and analyzed 7 d later.

Flow cytometry. Cells were stained with the following fluorochrome- or biotin-conjugated antibodies obtained from eBioscience (or another manufacturer, as indicated): anti-CD11c (N418), MHC II (M5/114.15.2), CD11b (M1/70), CD8α (53–6.7), Gr-1 (RB6-8C5), TCRβ (H57-597), CD3 (17A2), B220 (RA3-6B2), NK1.1 (PK136), Ter119 (TER-119), CD49b (DX5), CD4 (RM4-5 and GK1.5), FoxP3 (FJK-16s), CD24 (M1/69), Flt3 (A2F10), c-Kit (2B8), Sca-1 (D7), CD115 (AFS98), IL7-Rα (A7R34), CD45.1 (A20), CD45.2 (104), PD-L1 (MIH5), CD86 (GL1), DEC205 (NLDC-145; BioLegend), mPDCA-1/Bst2 (Miltenyi Biotec), Sirpα (P84, BD), CD80 (16-10A1), CD40 (1C10), and MHC I (AF6-88.5.5.3). Intracellular staining of FoxP3 was performed per the manufacturer's instructions (eBioscience). Cell acquisition was done on LSR II or LSR Fortessa (BD) and analysis was done using FlowJo (Tree Star).

For sorting, spleens were harvested from *Flt3*$^{+/+}$ or *Flt3*$^{ITD/+}$ FVB-B6 F_1 mice and sorted on either FACSAria (BD) or MoFlo (Beckman Coulter) instruments. DC populations were sorted as follows: pDC (Bst2$^+$ B220$^+$), cDCs (CD11c^{hi} MHCII$^+$ B220$^-$) and subsets thereof; canonical CD8$^+$ (CD8$^+$ SSC^{hi} DEC205$^+$ or CD86$^+$); noncanonical CD8$^+$ (CD8$^+$ SSC^{lo} DEC205$^-$ or CD86$^-$); Esam^{hi} (CD11b$^+$ Esam^{hi}); and Esam^{lo} (CD11b$^+$ Esam^{lo}).

Competitive chimeras. Recipient animals represented F_1 progeny of 129SvEvTac and B6.SJL mice (Taconic). Lethally irradiated (129xB6.SJL) F_1 recipients (CD45.1$^+$/CD45.2$^+$) were injected i.v. with a mixture of 10^6 B6.SJL (CD45.1$^+$) BM cells and 10^6 *Flt3*$^{+/+}$, *Flt3*$^{ITD/+}$, or *Flt3*$^{ITD/ITD}$ (CD45.2$^+$) BM cells.

Flt3L administration. *Cx$_3$cr1*$^{GFP/GFP}$ mice were injected i.p. with PBS or 5 μg recombinant Flt3L-Fc (LakePharma) every 3 d (days 0, 3, and 6) and analyzed on day 9 after initial treatment.

BrdU analysis. *Flt3*$^{+/+}$ or *Flt3*$^{ITD/+}$ mice were pulsed with an initial intraperitoneal injection with 1 mg BrdU (Sigma-Aldrich), followed by a continuous administration of 0.8 mg/ml BrdU in the drinking water for 2 d. Spleens were harvested after 2 d, treated with collagenase D (1 mg/ml) and DNase I (20 μg/ml), and analyzed for BrdU incorporation using the APC BrdU Flow kit (BD) per the manufacturer's instructions.

RNA isolation and gene expression analysis. Cells were sorted from splenocytes pooled from two to three animals of each genotype, and samples from independent experiments were used as biological replicates in RNA-Seq (three for CD8$^+$ cDCs, two for CD11b$^+$ cDCs, and two for pDCs). Sorted cells (3–5 × 10^3) were pelleted or sorted directly into TRIzol reagent (Thermo Fisher Scientific), and RNA was extracted using the Arcturus PicoPure kit (Thermo Fisher Scientific). For TRIzol samples, equal volume of 70% ethanol was added to the aqueous phase of TRIzol samples and applied to columns from the PicoPure kit. Up to 250 μl of ethanol/aqueous phase mix was loaded onto the column and spun at 100 *g* for 2 min for each load. Bound RNA was washed, treated with DNase I (QIAGEN), and eluted as per the manufacturer's instructions. To remove phenol contamination, eluate was resuspended in 100 μl of Wash Buffer 1 and reloaded onto a fresh column followed by elution.

cDNA libraries were prepared using the SMART-seq v4 Ultra Low Input RNA kit and Low Input Library Prep kit (Life Sciences) and were sequenced on an Illumina HiSeq 2500. Reads were mapped to *Mus musculus* mm10 genome using FastQ Groomer (v1.0.4) and Bowtie2 (v0.4) within the Galaxy platform (Giardine et al., 2005; Blankenberg et al., 2010; Langmead and Salzberg, 2012). Principal component analysis and identification of differentially expressed genes were performed using DESeq2 (Love et al., 2014). Differential expression was selected based on an adjusted p-value of <0.1 (false discovery rate of 10%), exhibiting at least a twofold difference in expression levels ($\log_2$ fold change ≥1) and $P < 0.05$ for statistical significance. Principal component analysis was performed using calculated transformed counts (regularized logarithm) calculated by the DESeq2 package. Plots were generated using the R Studio software package.

***Lm* infection.** Mice were infected with 5 × 10^3 CFU of *Lm* expressing OVA in PBS and injected i.v. For bacterial titration, spleens were weighed and then pressed into nylon strainers to make single-cell suspensions in sterile PBS. Cells were lysed with an equal volume of sterile water with 0.1% Triton X-100 and plated on brain–heart infusion agar plates (Difco; BD) for overnight incubation at 37°C. Colonies were counted the next day.

Lymphopenia-induced homeostatic proliferation. Spleen and LNs were isolated from *FoxP3*^{GFP} reporter mice and T cells were enriched on MACS columns (Miltenyi Biotec) by negative selection with antibodies against CD11b, CD11c, B220, Gr-1, CD49b, and Ter119. T cells were stained with 5 μM CTV (Life Technologies) in PBS for 20 min at 37°C, washed, and injected i.v. into *Rag1*$^{-/-}$ *Flt3*$^{+/+}$or *Rag1*$^{-/-}$ *Flt3*$^{ITD/+}$ recipients (2 × 10^6 per mouse). Splenocytes from the recipients were analyzed 5 d later.

Allogeneic MLR. Splenic DCs were prepared from (B6x-FVB) F_1 *Flt3*$^{+/+}$ or *Flt3*$^{ITD/+}$ littermates by positive selection using biotinylated anti-CD11c, streptavidin microbeads, and MACS columns (Miltenyi Biotec). T cells from *FoxP3*$^{GFP/GFP}$ spleen and LNs were enriched by magnetic negative selection and labeled with CTV as above. Labeled T cells were plated in a 96-well plate (5 × 10^4/well) in RPMI/10% FCS with the indicated numbers of CD11c-enriched stimulator cells and cultured for 4 d.

T reg cell depletion. *FoxP3*$^{DTR\text{-}GFP/y}$ *Flt3*$^{+/+}$ and *FoxP3*$^{DTR\text{-}GFP/y}$ *Flt3*$^{ITD/+}$ mice were injected i.p. with 50 μg/kg DT (Sigma-Aldrich) on two consecutive days. Blood was analyzed for the

presence of GFP^+ T reg cells on days 0 (before treatment), 2, 10, 14, 21, and 28, and the mice were sacrificed and analyzed on day 28 after injection.

Accession number. RNA-seq data are available in the NCBI Gene Expression Omnibus database under the accession no. GSE76132.

Acute graft-versus-host response. Spleen and LNs were isolated from C57BL/6 ($H\text{-}2^b$; CD45.2) mice, pooled, and injected i.v. (3×10^7 cells/mouse) into nonirradiated (B6xFVB) F_1 recipients ($H\text{-}2^b/H\text{-}2^q$; CD45.2/CD45.1). Spleens were harvested and analyzed 1 wk later. For antibody blockade studies, 200 µg of control IgG, anti-mPD-L1 (10F.9G2), or anti-mPD-1 (RMP1-14) were injected i.p. on the same day before graft transfer on days 0, 2, and 5, and analyzed on day 7 or 8.

Online supplemental material. Fig. S1 shows the definition of DC progenitor populations. Fig. S2 shows the definition of DC progenitors in *Flt3*$^{ITD/ITD}$ mice. A supplemental dataset, available as an Excel file, shows differentially expressed genes between *Flt3*$^{ITD/+}$ and *Flt3*$^{+/+}$ cells in each DC subset. Online supplemental material is available at http://www.jem.org/cgi/content/full/jem.20150642/DC1.

ACKNOWLEDGMENTS

We thank K. Liu, I. Ivanov, K. Sawai, K. Lewis, X.Y. Qu, M. Warren, M.R. Smith-Raska and S. Weisberg for advice and support.

This work was supported by the National Institutes of Health (NIH) grant AI072571 (B. Reizis) and training grants CA009503 and AI100853 (C.M. Lau). Cell sorting was performed at the CCTI Flow Cytometry Core, which is supported in part by NIH grant OD020056. Additional cell sorting was performed at the New York University Cytometry and Cell Sorting Core, and preparation of cDNA libraries and sequencing was performed at the New York University Genome Tech Center, both of which are supported by NIH grant CA016087.

The authors declare no competing financial interests.

Submitted: 8 April 2015

Accepted: 20 January 2016

REFERENCES

Adolfsson, J., O.J. Borge, D. Bryder, K. Theilgaard-Mönch, I. Astrand-Grundström, E. Sitnicka, Y. Sasaki, and S.E. Jacobsen. 2001. Upregulation of Flt3 expression within the bone marrow $Lin^-Sca1^+c\text{-}kit^+$ stem cell compartment is accompanied by loss of self-renewal capacity. *Immunity.* 15:659–669. http://dx.doi.org/10.1016/S1074-7613(01)00220-5

Anandasabapathy, N., R. Feder, S. Mollah, S.W. Tse, M.P. Longhi, S. Mehandru, I. Matos, C. Cheong, D. Ruane, L. Brane, et al. 2014. Classical Flt3L-dependent dendritic cells control immunity to protein vaccine. *J. Exp. Med.* 211:1875–1891. http://dx.doi.org/10.1084/jem.20131397

Bachanova, V., S. Cooley, T.E. Defor, M.R. Verneris, B. Zhang, D.H. McKenna, J. Curtsinger, A. Panoskaltsis-Mortari, D. Lewis, K. Hippen, et al. 2014. Clearance of acute myeloid leukemia by haploidentical natural killer cells is improved using IL-2 diphtheria toxin fusion protein. *Blood.* 123:3855–3863. http://dx.doi.org/10.1182/blood-2013-10-532531

Bailey, E.J., A.S. Duffield, S.M. Greenblatt, P.D. Aplan, and D. Small. 2013. Effect of FLT3 ligand on survival and disease phenotype in murine models harboring a FLT3 internal tandem duplication mutation. *Comp. Med.* 63:218–226.

Bar-On, L., T. Birnberg, K.L. Lewis, B.T. Edelson, D. Bruder, K. Hildner, J. Buer, K.M. Murphy, B. Reizis, and S. Jung. 2010. $CX3CR1^+$ $CD8\alpha^+$ dendritic cells are a steady-state population related to plasmacytoid dendritic cells. *Proc. Natl. Acad. Sci. USA.* 107:14745–14750. http://dx.doi.org/10.1073/pnas.1001562107

Bar-On, L., T. Birnberg, K.W. Kim, and S. Jung. 2011. Dendritic cell-restricted CD80/86 deficiency results in peripheral regulatory T-cell reduction but is not associated with lymphocyte hyperactivation. *Eur. J. Immunol.* 41:291–298. http://dx.doi.org/10.1002/eji.201041169

Blankenberg, D., G. Von Kuster, N. Coraor, G. Ananda, R. Lazarus, M. Mangan, A. Nekrutenko, and J. Taylor. 2010. Galaxy: a web-based genome analysis tool for experimentalists. *Curr Protoc Mol Biol.* Chapter 19:Unit 19 10 11-21.

Blazar, B.R., B.M. Carreno, A. Panoskaltsis-Mortari, L. Carter, Y. Iwai, H. Yagita, H. Nishimura, and P.A. Taylor. 2003. Blockade of programmed death-1 engagement accelerates graft-versus-host disease lethality by an IFN-γ-dependent mechanism. *J. Immunol.* 171:1272–1277. http://dx.doi.org/10.4049/jimmunol.171.3.1272

Brasel, K., H.J. McKenna, P.J. Morrissey, K. Charrier, A.E. Morris, C.C. Lee, D.E. Williams, and S.D. Lyman. 1996. Hematologic effects of flt3 ligand in vivo in mice. *Blood.* 88:2004–2012.

Breton, G., J. Lee, Y.J. Zhou, J.J. Schreiber, T. Keler, S. Puhr, N. Anandasabapathy, S. Schlesinger, M. Caskey, K. Liu, and M.C. Nussenzweig. 2015. Circulating precursors of human $CD1c^+$ and $CD141^+$ dendritic cells. *J. Exp. Med.* 212:401–413. http://dx.doi.org/10.1084/jem.20141441

Cancer Genome Atlas Research Network. 2013. Genomic and epigenomic landscapes of adult de novo acute myeloid leukemia. *N. Engl. J. Med.* 368:2059–2074. http://dx.doi.org/10.1056/NEJMoa1301689

Chilton, P.M., F. Rezzoug, I. Fugier-Vivier, L.A. Weeter, H. Xu, Y. Huang, M.B. Ray, and S.T. Ildstad. 2004. Flt3-ligand treatment prevents diabetes in NOD mice. *Diabetes.* 53:1995–2002. http://dx.doi.org/10.2337/diabetes.53.8.1995

Chu, S.H., D. Heiser, L. Li, I. Kaplan, M. Collector, D. Huso, S.J. Sharkis, C. Civin, and D. Small. 2012. FLT3-ITD knockin impairs hematopoietic stem cell quiescence/homeostasis, leading to myeloproliferative neoplasm. *Cell Stem Cell.* 11:346–358. http://dx.doi.org/10.1016/j.stem.2012.05.027

Collins, C.B., C.M. Aherne, E.N. McNamee, M.D. Lebsack, H. Eltzschig, P. Jedlicka, and J. Rivera-Nieves. 2012. Flt3 ligand expands $CD103^+$ dendritic cells and $FoxP3^+$ T regulatory cells, and attenuates Crohn's-like murine ileitis. *Gut.* 61:1154–1162. http://dx.doi.org/10.1136/gutjnl-2011-300820

Darrasse-Jèze, G., S. Deroubaix, H. Mouquet, G.D. Victora, T. Eisenreich, K.H. Yao, R.F. Masilamani, M.L. Dustin, A. Rudensky, K. Liu, and M.C. Nussenzweig. 2009. Feedback control of regulatory T cell homeostasis by dendritic cells in vivo. *J. Exp. Med.* 206:1853–1862. http://dx.doi.org/10.1084/jem.20090746

Ding, L., T.J. Ley, D.E. Larson, C.A. Miller, D.C. Koboldt, J.S. Welch, J.K. Ritchey, M.A. Young, T. Lamprecht, M.D. McLellan, et al. 2012. Clonal evolution in relapsed acute myeloid leukaemia revealed by whole-genome sequencing. *Nature.* 481:506–510. http://dx.doi.org/10.1038/nature10738

Edelson, B.T., T.R. Bradstreet, K. Hildner, J.A. Carrero, K.E. Frederick, W. Kc, R. Belizaire, T. Aoshi, R.D. Schreiber, M.J. Miller, et al.. 2011. $CD8\alpha^+$ dendritic cells are an obligate cellular entry point for productive infection by *Listeria monocytogenes*. *Immunity.* 35:236–248. http://dx.doi.org/10.1016/j.immuni.2011.06.012

Fontenot, J.D., J.P. Rasmussen, L.M. Williams, J.L. Dooley, A.G. Farr, and A.Y. Rudensky. 2005. Regulatory T cell lineage specification by the forkhead transcription factor foxp3. *Immunity.* 22:329–341. http://dx.doi.org/10.1016/j.immuni.2005.01.016

Geissmann, F., M.G. Manz, S. Jung, M.H. Sieweke, M. Merad, and K. Ley. 2010. Development of monocytes, macrophages, and dendritic cells. *Science.* 327:656–661. http://dx.doi.org/10.1126/science.1178331

Giardine, B., C. Riemer, R.C. Hardison, R. Burhans, L. Elnitski, P. Shah, Y. Zhang, D. Blankenberg, I. Albert, J. Taylor, et al. 2005. Galaxy: a platform for interactive large-scale genome analysis. *Genome Res.* 15:1451–1455. http://dx.doi.org/10.1101/gr.4086505

Ginhoux, F., K. Liu, J. Helft, M. Bogunovic, M. Greter, D. Hashimoto, J. Price, N. Yin, J. Bromberg, S.A. Lira, et al.. 2009. The origin and development of nonlymphoid tissue $CD103^+$ DCs. *J. Exp. Med.* 206:3115–3130. http://dx.doi.org/10.1084/jem.20091756

Govindaraj, C., P. Tan, P. Walker, A. Wei, A. Spencer, and M. Plebanski. 2014. Reducing TNF receptor 2^+ regulatory T cells via the combined action of azacitidine and the HDAC inhibitor, panobinostat for clinical benefit in acute myeloid leukemia patients. *Clin. Cancer Res.* 20:724–735. http://dx.doi.org/10.1158/1078-0432.CCR-13-1576

Hildner, K., B.T. Edelson, W.E. Purtha, M. Diamond, H. Matsushita, M. Kohyama, B. Calderon, B.U. Schraml, E.R. Unanue, M.S. Diamond, et al.. 2008. Batf3 deficiency reveals a critical role for $CD8\alpha^+$ dendritic cells in cytotoxic T cell immunity. *Science.* 322:1097–1100. http://dx.doi.org/10.1126/science.1164206

Jan, M., T.M. Snyder, M.R. Corces-Zimmerman, P. Vyas, I.L. Weissman, S.R. Quake, and R. Majeti. 2012. Clonal evolution of preleukemic hematopoietic stem cells precedes human acute myeloid leukemia. *Sci. Transl. Med.* 4:149ra118. http://dx.doi.org/10.1126/scitranslmed.3004315

Jung, S., J. Aliberti, P. Graemmel, M.J. Sunshine, G.W. Kreutzberg, A. Sher, and D.R. Littman. 2000. Analysis of fractalkine receptor CX(3)CR1 function by targeted deletion and green fluorescent protein reporter gene insertion. *Mol. Cell. Biol.* 20:4106–4114. http://dx.doi.org/10.1128/MCB.20.11.4106-4114.2000

Karsunky, H., M. Merad, A. Cozzio, I.L. Weissman, and M.G. Manz. 2003. Flt3 ligand regulates dendritic cell development from $Flt3^+$ lymphoid and myeloid-committed progenitors to $Flt3^+$ dendritic cells in vivo. *J. Exp. Med.* 198:305–313. http://dx.doi.org/10.1084/jem.20030323

Kharazi, S., A.J. Mead, A. Mansour, A. Hultquist, C. Böiers, S. Luc, N. Buza-Vidas, Z. Ma, H. Ferry, D. Atkinson, et al. 2011. Impact of gene dosage, loss of wild-type allele, and FLT3 ligand on Flt3-ITD-induced myeloproliferation. *Blood.* 118:3613–3621. http://dx.doi.org/10.1182/blood-2010-06-289207

Kim, J.M., J.P. Rasmussen, and A.Y. Rudensky. 2007. Regulatory T cells prevent catastrophic autoimmunity throughout the lifespan of mice. *Nat. Immunol.* 8:191–197. http://dx.doi.org/10.1038/ni1428

Kindler, T., D.B. Lipka, and T. Fischer. 2010. FLT3 as a therapeutic target in AML: still challenging after all these years. *Blood.* 116:5089–5102. http://dx.doi.org/10.1182/blood-2010-04-261867

Klein, O., L.M. Ebert, D. Zanker, K. Woods, B.S. Tan, J. Fucikova, A. Behren, I.D. Davis, E. Maraskovsky, W. Chen, and J. Cebon. 2013. Flt3 ligand expands $CD4^+$ $FoxP3^+$ regulatory T cells in human subjects. *Eur. J. Immunol.* 43:533–539. http://dx.doi.org/10.1002/eji.201242603

Langmead, B., and S.L. Salzberg. 2012. Fast gapped-read alignment with Bowtie 2. *Nat. Methods.* 9:357–359. http://dx.doi.org/10.1038/nmeth.1923

Laouar, Y., T. Welte, X.Y. Fu, and R.A. Flavell. 2003. STAT3 is required for Flt3L-dependent dendritic cell differentiation. *Immunity.* 19:903–912. http://dx.doi.org/10.1016/S1074-7613(03)00332-7

Lee, B.H., Z. Tothova, R.L. Levine, K. Anderson, N. Buza-Vidas, D.E. Cullen, E.P. McDowell, J. Adelsperger, S. Fröhling, B.J.P. Huntly, et al. 2007. FLT3 mutations confer enhanced proliferation and survival properties to multipotent progenitors in a murine model of chronic myelomonocytic leukemia. *Cancer Cell.* 12:367–380. http://dx.doi.org/10.1016/j.ccr.2007.08.031

Lewis, K.L., and B. Reizis. 2012. Dendritic cells: arbiters of immunity and immunological tolerance. *Cold Spring Harb. Perspect. Biol.* 4:a007401. http://dx.doi.org/10.1101/cshperspect.a007401

Lewis, K.L., M.L. Caton, M. Bogunovic, M. Greter, L.T. Grajkowska, D. Ng, A. Klinakis, I.F. Charo, S. Jung, J.L. Gommerman, et al. 2011. Notch2 receptor signaling controls functional differentiation of dendritic cells in the spleen and intestine. *Immunity.* 35:780–791. http://dx.doi.org/10.1016/j.immuni.2011.08.013

Li, L., L. Huang, H. Ye, S.P. Song, A. Bajwa, S.J. Lee, E.K. Moser, K. Jaworska, G.R. Kinsey, Y.J. Day, et al. 2012. Dendritic cells tolerized with adenosine A_2AR agonist attenuate acute kidney injury. *J. Clin. Invest.* 122:3931–3942. http://dx.doi.org/10.1172/JCI63170

Liu, K., and M.C. Nussenzweig. 2010. Origin and development of dendritic cells. *Immunol. Rev.* 234:45–54. http://dx.doi.org/10.1111/j.0105-2896.2009.00879.x

Liu, K., C. Waskow, X. Liu, K. Yao, J. Hoh, and M. Nussenzweig. 2007. Origin of dendritic cells in peripheral lymphoid organs of mice. *Nat. Immunol.* 8:578–583. http://dx.doi.org/10.1038/ni1462

Love, M.I., W. Huber, and S. Anders. 2014. Moderated estimation of fold change and dispersion for RNA-seq data with DESeq2. *Genome Biol.* 15:550. http://dx.doi.org/10.1186/s13059-014-0550-8

Maldonado, R.A., and U.H. von Andrian. 2010. How tolerogenic dendritic cells induce regulatory T cells. *Adv. Immunol.* 108:111–165. http://dx.doi.org/10.1016/B978-0-12-380995-7.00004-5

Maraskovsky, E., K. Brasel, M. Teepe, E.R. Roux, S.D. Lyman, K. Shortman, and H.J. McKenna. 1996. Dramatic increase in the numbers of functionally mature dendritic cells in Flt3 ligand-treated mice: multiple dendritic cell subpopulations identified. *J. Exp. Med.* 184:1953–1962. http://dx.doi.org/10.1084/jem.184.5.1953

Maraskovsky, E., E. Daro, E. Roux, M. Teepe, C.R. Maliszewski, J. Hoek, D. Caron, M.E. Lebsack, and H.J. McKenna. 2000. In vivo generation of human dendritic cell subsets by Flt3 ligand. *Blood.* 96:878–884.

McKenna, H.J., K.L. Stocking, R.E. Miller, K. Brasel, T. De Smedt, E. Maraskovsky, C.R. Maliszewski, D.H. Lynch, J. Smith, B. Pulendran, et al. 2000. Mice lacking flt3 ligand have deficient hematopoiesis affecting hematopoietic progenitor cells, dendritic cells, and natural killer cells. *Blood.* 95:3489–3497.

Mead, A.J., S. Kharazi, D. Atkinson, I. Macaulay, C. Pecquet, S. Loughran, M. Lutteropp, P. Woll, O. Chowdhury, S. Luc, et al. 2013. FLT3-ITDs instruct a myeloid differentiation and transformation bias in lymphomyeloid multipotent progenitors. *Cell Reports.* 3:1766–1776. http://dx.doi.org/10.1016/j.celrep.2013.04.031

Merad, M., P. Sathe, J. Helft, J. Miller, and A. Mortha. 2013. The dendritic cell lineage: ontogeny and function of dendritic cells and their subsets in the steady state and the inflamed setting. *Annu. Rev. Immunol.* 31:563–604. http://dx.doi.org/10.1146/annurev-immunol-020711-074950

O'Keeffe, M., H. Hochrein, D. Vremec, J. Pooley, R. Evans, S. Woulfe, and K. Shortman. 2002. Effects of administration of progenipoietin 1, Flt-3 ligand, granulocyte colony-stimulating factor, and pegylated granulocyte-macrophage colony-stimulating factor on dendritic cell subsets in mice. *Blood.* 99:2122–2130. http://dx.doi.org/10.1182/blood.V99.6.2122

Parcells, B.W., A.K. Ikeda, T. Simms-Waldrip, T.B. Moore, and K.M. Sakamoto. 2006. FMS-like tyrosine kinase 3 in normal hematopoiesis and acute myeloid leukemia. *Stem Cells.* 24:1174–1184. http://dx.doi.org/10.1634/stemcells.2005-0519

Rickmann, M., J. Krauter, K. Stamer, M. Heuser, G. Salguero, E. Mischak-Weissinger, A. Ganser, and R. Stripecke. 2011. Elevated frequencies of leukemic myeloid and plasmacytoid dendritic cells in acute myeloid leukemia with the FLT3 internal tandem duplication. *Ann. Hematol.* 90:1047–1058. http://dx.doi.org/10.1007/s00277-011-1231-2

Rickmann, M., L. Macke, B.S. Sundarasetty, K. Stamer, C. Figueiredo, R. Blasczyk, M. Heuser, J. Krauter, A. Ganser, and R. Stripecke. 2013. Monitoring dendritic cell and cytokine biomarkers during remission prior to relapse in patients with FLT3-ITD acute myeloid leukemia. *Ann. Hematol.* 92:1079–1090. http://dx.doi.org/10.1007/s00277-013-1744-y

Rullé, S., M.D. Ah Kioon, C. Asensio, J. Mussard, H.K. Ea, M.C. Boissier, F. Lioté, and G. Falgarone. 2012. Adrenomedullin, a neuropeptide with immunoregulatory properties induces semi-mature tolerogenic dendritic cells. *Immunology.* 136:252–264. http://dx.doi.org/10.1111/j.1365-2567.2012.03577.x

Sathaliyawala, T., W.E. O'Gorman, M. Greter, M. Bogunovic, V. Konjufca, Z.E. Hou, G.P. Nolan, M.J. Miller, M. Merad, and B. Reizis. 2010. Mammalian target of rapamycin controls dendritic cell development downstream of Flt3 ligand signaling. *Immunity.* 33:597–606. http://dx.doi.org/10.1016/j.immuni.2010.09.012

Schick, J., V. Vogt, M. Zerwes, T. Kroell, D. Kraemer, C.H. Köhne, A. Hausmann, R. Buhmann, J. Tischer, and H. Schmetzer. 2013. Antileukemic T-cell responses can be predicted by the composition of specific regulatory T-cell subpopulations. *J. Immunother.* 36:223–237. http://dx.doi.org/10.1097/CJI.0b013e31829180e7

Sela, U., P. Olds, A. Park, S.J. Schlesinger, and R.M. Steinman. 2011. Dendritic cells induce antigen-specific regulatory T cells that prevent graft versus host disease and persist in mice. *J. Exp. Med.* 208:2489–2496. http://dx.doi.org/10.1084/jem.20110466

Sen, B., S. Peng, D.M. Woods, I. Wistuba, D. Bell, A.K. El-Naggar, S.Y. Lai, and F.M. Johnson. 2012. STAT5A-mediated SOCS2 expression regulates Jak2 and STAT3 activity following c-Src inhibition in head and neck squamous carcinoma. *Clin. Cancer Res.* 18:127–139. http://dx.doi.org/10.1158/1078-0432.CCR-11-1889

Shlush, L.I., S. Zandi, A. Mitchell, W.C. Chen, J.M. Brandwein, V. Gupta, J.A. Kennedy, A.D. Schimmer, A.C. Schuh, K.W. Yee, et al. HALT Pan-Leukemia Gene Panel Consortium. 2014. Identification of pre-leukaemic haematopoietic stem cells in acute leukaemia. *Nature.* 506:328–333. http://dx.doi.org/10.1038/nature13038

Sitnicka, E., N. Buza-Vidas, S. Larsson, J.M. Nygren, K. Liuba, and S.E. Jacobsen. 2003. Human CD34$^+$ hematopoietic stem cells capable of multilineage engrafting NOD/SCID mice express flt3: distinct flt3 and c-kit expression and response patterns on mouse and candidate human hematopoietic stem cells. *Blood.* 102:881–886. http://dx.doi.org/10.1182/blood-2002-06-1694

Small, D. 2006. FLT3 mutations: biology and treatment. *Hematology (Am Soc Hematol Educ Program).* 2006:178–184. http://dx.doi.org/10.1182/asheducation-2006.1.178

Smith, C.C., Q. Wang, C.S. Chin, S. Salerno, L.E. Damon, M.J. Levis, A.E. Perl, K.J. Travers, S. Wang, J.P. Hunt, et al. 2012. Validation of ITD mutations in FLT3 as a therapeutic target in human acute myeloid leukaemia. *Nature.* 485:260–263. http://dx.doi.org/10.1038/nature11016

Steinman, R.M., D. Hawiger, and M.C. Nussenzweig. 2003. Tolerogenic dendritic cells. *Annu. Rev. Immunol.* 21:685–711. http://dx.doi.org/10.1146/annurev.immunol.21.120601.141040

Svensson, M.N., S.E. Andersson, M.C. Erlandsson, I.M. Jonsson, A.K. Ekwall, K.M. Andersson, A. Nilsson, L. Bian, M. Brisslert, and M.I. Bokarewa. 2013. Fms-like tyrosine kinase 3 ligand controls formation of regulatory T cells in autoimmune arthritis. *PLoS One.* 8:e54884. http://dx.doi.org/10.1371/journal.pone.0054884

Swee, L.K., N. Bosco, B. Malissen, R. Ceredig, and A. Rolink. 2009. Expansion of peripheral naturally occurring T regulatory cells by Fms-like tyrosine kinase 3 ligand treatment. *Blood.* 113:6277–6287. http://dx.doi.org/10.1182/blood-2008-06-161026

Swords, R., C. Freeman, and F. Giles. 2012. Targeting the FMS-like tyrosine kinase 3 in acute myeloid leukemia. *Leukemia.* 26:2176–2185. http://dx.doi.org/10.1038/leu.2012.114

Takada, K., and S.C. Jameson. 2009. Naive T cell homeostasis: from awareness of space to a sense of place. *Nat. Rev. Immunol.* 9:823–832. http://dx.doi.org/10.1038/nri2657

Varol, C., A. Vallon-Eberhard, E. Elinav, T. Aychek, Y. Shapira, H. Luche, H.J. Fehling, W.D. Hardt, G. Shakhar, and S. Jung. 2009. Intestinal lamina propria dendritic cell subsets have different origin and functions. *Immunity.* 31:502–512. http://dx.doi.org/10.1016/j.immuni.2009.06.025

Waskow, C., K. Liu, G. Darrasse-Jèze, P. Guermonprez, F. Ginhoux, M. Merad, T. Shengelia, K. Yao, and M. Nussenzweig. 2008. The receptor tyrosine kinase Flt3 is required for dendritic cell development in peripheral lymphoid tissues. *Nat. Immunol.* 9:676–683. http://dx.doi.org/10.1038/ni.1615

Yang, W., and Y. Xu. 2013. Clinical significance of Treg cell frequency in acute myeloid leukemia. *Int. J. Hematol.* 98:558–562. http://dx.doi.org/10.1007/s12185-013-1436-3

Zaiss, D.M., W.C. Gause, L.C. Osborne, and D. Artis. 2015. Emerging functions of amphiregulin in orchestrating immunity, inflammation, and tissue repair. *Immunity.* 42:216–226. http://dx.doi.org/10.1016/j.immuni.2015.01.020

Zelenay, S., A.G. van der Veen, J.P. Böttcher, K.J. Snelgrove, N. Rogers, S.E. Acton, P. Chakravarty, M.R. Girotti, R. Marais, S.A. Quezada, et al.. 2015. Cyclooxygenase-dependent tumor growth through evasion of immunity. *Cell.* 162:1257–1270. http://dx.doi.org/10.1016/j.cell.2015.08.015

Zheng, R., E. Bailey, B. Nguyen, X. Yang, O. Piloto, M. Levis, and D. Small. 2011. Further activation of FLT3 mutants by FLT3 ligand. *Oncogene.* 30:4004–4014. http://dx.doi.org/10.1038/onc.2011.110